

Self-organized criticality within generalized Lorenz scheme

Alexander I. Olemskoi *

Max-Planck-Institut für Physik komplexer Systeme, Nöthnitzer Strasse 38, D-01187 Dresden, Germany

Alexei V. Khomenko †

Sumy State University, Rimskii-Korsakov St. 2, 40007 Sumy, Ukraine

Dmitrii O. Kharchenko ‡

Max-Planck-Institut für Physik komplexer Systeme, Nöthnitzer Strasse 38, D-01187 Dresden, Germany

(November 2, 2018)

The theory of a flux steady-state related to avalanche formation is presented for the simplest model of a sand pile within framework of the Lorenz approach. The stationary values of sand velocity and sand pile slope are derived as functions of control parameter (driven sand pile slope). The additive noises of above values are introduced to build the phase diagram, where the noise intensities determine both avalanche and non-avalanche domains, as well as mixed one. Being corresponded to the SOC regime, the last domain is crucial to affect of the noise intensities of vertical component of sand velocity and sand pile slope especially. To address to a self-similar behavior, a fractional feedback is used as efficient ingredient of the modified Lorenz system. In a spirit of Edwards paradigm, an effective thermodynamics is introduced to determine a distribution over avalanche ensemble with negative temperature. Steady-state behavior of the moving grains number, as well as nonextensive values of entropy and energy is studied in detail. The power-law distribution over avalanche sizes is described within a fractional Lorenz scheme, where noise of the energy plays a crucial role. This distribution is shown to be solution of both fractional Fokker-Planck equation and nonlinear one. As a result, we obtain new relations between exponent of the size distribution, fractal dimension of phase space, characteristic exponent of multiplicative noise, number of governing equations, dynamical exponents and nonextensivity parameter.

PACS number(s): 05.45.-a, 05.65.+b, 45.70.-n, 64.60.Ht

*Present address: Sumy State University, Rimskii-Korsakov St. 2, 40007 Sumy, Ukraine; electronic address: olemskoi@ssu.sumy.ua

†Electronic address: khom@phe.ssu.sumy.ua

‡Present address: Sumy State University, Rimskii-Korsakov St. 2, 40007 Sumy, Ukraine; electronic address: dikh@ssu.sumy.ua

I. INTRODUCTION

In recent years considerable study has been given to the theory of self-organized criticality (SOC) that explains spontaneous (avalanche-type) dynamics, unlike the typical phase transitions that occur only when a control parameter is driven to a critical value [1], [2]. A main feature of the systems displaying SOC is their self-similarity that derives to a power-law distribution over avalanche sizes. Respectively, SOC models are mostly studied by making use of the scaling-type arguments supplemented with extensive computer simulations (see [3]). On the contrary, in this paper we put forward an analytical approach, which is enable to describe in phenomenological manner both process of a single avalanche formation and behavior of whole avalanche ensemble.

The SOC behavior appears in vast variety of systems such as a real sand pile (ensemble of grains of sand moving along increasingly tilted surface) [4] – [7], intermittency in biological evolution [8], earthquakes and forest-fires, depinning transitions in random medium and so on (see [9]). Among the above models the sandpile is the simplest and most widely studied as analytically [10], [11], so numerically [12] – [14]. In analytical direction, a variety of field theory approaches is worthwhile to notice. Among them, the field scheme [15] based on nonlinear diffusion equation has failed to account for the main feature of self-organizing systems – the self-consistent character of avalanche dynamics. The visible reason is that using one-parameter approach does not take into account a feedback between open subsystem and environment that are related to order and control parameters, respectively (see criticism in Refs. [5], [6] also). Much more substantial picture is given within two-parameter approaches [5] – [7], [16] that use both fundamental fields: gauge ones related to hydrodynamical modes type of sand pile height and material fields as a number of moving sand grains (avalanche size). Making use of the mean-field approximation shows that the self-similar regime of the sand pile dynamics is relevant to subcritical behavior, where a characteristic time of the order parameter variation is much more than the same for the control parameter, and the latter follows the former adiabatically. Such type adiabatic behavior is inherent in usual regime of system evolving in course of phase transitions [17] and jammed motion of vehicles [18], so that adiabatic approach will be put on basis of our consideration.

Perfect treatment of the SOC has been achieved within three-parameter approach based on the Reggeon field theory that uses the density of active sites ρ_a as the order parameter and conserved field of the energy density ζ as the control parameter [19], [20]. Along this line, SOC regime appears as a result of competition between a rate of the energy input $h > 0$ and a dissipation rate ϵ . It is appeared that the system under consideration behaves in quite different manner in case of fixed energy, when $h = \epsilon = 0$ and total energy is conserved, and for driven sandpile, when $h \rightarrow 0^+$, $\epsilon \rightarrow 0$ at stationarity condition $\epsilon > h$. The first case shows [19], [20] to be reduced to the picture of supercritical regime, where nonhomogeneity of initial distribution of energy arrives at a non-Markovian term and space-dependent parameters of theory. At dimensions above critical value $d_c = 4$, this case is found to be identical to the simplest Landau picture with $\rho_a \sim \zeta - \zeta_c$ in active stationary state ($\zeta > \zeta_c$) and $\rho_a = 0$ in absorbing configuration ($\zeta < \zeta_c$). Fundamentally different picture appears in the case of driven sandpile, where due to external input $h \rightarrow 0^+$ the energy density is lost as an independent field being reduced to the critical value ζ_c . Here, the average magnitude of

the density of active sites is equal $\langle \rho_a \rangle = h/\epsilon$, so that the susceptibility $\chi \equiv \langle \partial \rho_a / \partial h \rangle$ is turned out to be $\chi = \epsilon^{-1}$. Respectively, a response function behaves at large distances r as $\chi(r) \sim r^{2-d} e^{-r/\xi}$, where d is a space dimension, $\xi \sim \epsilon^{-1/2}$ is a correlation length being scale of a system size $L \sim \epsilon^{-1/\mu}$. It is remarkable that such mean-field-type behavior is caused solely by stationary condition and translational invariance [20]. A set of basic critical exponents governing scaling avalanche formation reads [19]: $\beta = \gamma = \delta = 1$, $\mu = 2$, $\nu = 1/2$ and $\eta = 0$. On the other hand, scaling relations accompanied by equality of the susceptibility and mean size of avalanche yield the following expressions

$$\tau = 1 + \frac{z}{D}, \quad \tau = 2 \left(1 - \frac{1}{D} \right); \quad D = \frac{\mu}{\sigma} \quad (1)$$

for the exponents of the avalanche size distribution

$$P(s, \epsilon) = s^{-\tau} \mathcal{P}(x); \quad x \equiv s/s_c, \quad s_c \sim \epsilon^{-1/\sigma}, \quad (2)$$

where a critical size s_c is connected with system size $L \sim \xi$ and a characteristic time $t_c \sim L^z$ as $s_c \sim L^D \sim t_c^{D/z}$ (exponents $D = \mu/\sigma$ and z are fractal dimension and dynamical exponent related to a critical avalanche, respectively). According to Ref. [19], the mean-field magnitudes of the above exponents are as follows: $\tau = 3/2$, $\sigma = 1/2$, $D = 4$ and $z = 2$.

Along the standard approach [21], we will use as gauge, so material fields: being reduced to velocity components and sand pile slope, the formers are considered at study of a single avalanche formation, whereas the latters are reduced to the number of moving sand grains at examination of a distribution over avalanche sizes. Section II contains the self-consistent theory of the flux steady-state developed along the first direction. It enables us to treat the problem of a single avalanche formation on the basis of the unified analytical approach being relevant to the case of fixed energy in Refs. [20]. Section III deals with accounting additive noises of the sand velocity components and sand pile slope. The noise intensities increase is shown to make possible avalanche emergence even in non-driven systems. By this, the control parameter noise plays a crucial role. Such type fluctuational regime corresponds to the case $h \rightarrow 0^+$ [20], where a distribution of order parameter is appeared in an algebraic form with integer exponent. In order to be not restricted by such particular case, we introduce unified Lorenz system with fractional feedback in Section IV. Using this supposition allows us to describe subcritical regime of the avalanche formation in natural manner. The above generalization is put forward basis of Section V devoted to consideration of avalanche ensemble. Following famous Edwards paradigm [22], [23], an effective scheme addressed to nonextensive thermodynamics [24] is proposed to be determined by a time-dependent distribution over energies of moving sand grains. To generalize the Edwards scheme to nonstationary nonextensive system, we use the fractional Lorenz system, where the avalanche size plays a role of the order parameter, nonextensive complexity is reduced to the conjugate field and nonconserved energy of the moving grains is the control parameter. Within the framework of such approach, the phase diagram is built to define the different domains of system behavior as a function of noise intensities of above values. As a result, we arrive at natural conclusion that the power-law distribution (2) inherent in the SOC regime is caused by noise of the energy.

Section VI shows that this distribution is the solution of both nonlinear Fokker-Planck equation, which appears at studying nonextensive systems [24], and fractional Fokker-Planck

equation inherent in Lévy-type processes characterized by dynamical exponent z [25]. As a result, we obtain new relations between the exponent τ of the distribution (2), fractal dimension D of phase space, characteristic exponent of multiplicative noise, number of governing equations being needed to present self-consistent behavior in SOC regime, dynamical exponent z and Tsallis nonextensivity parameter q .

Section VIII is Appendix containing basic properties of fractional integral and derivative, as well as Jackson derivative.

II. NOISELESS AVALANCHE FORMATION

Within framework of the simplest model of a real sand pile, a dependence $y = y(t, x)$ defines its surface at given instant of time t . Locally the flow of sand can be described in terms of three quantities: the horizontal and vertical components of the sand velocity, $\dot{x} = \partial x / \partial t$, $\dot{y} = \partial y / \partial t$, and the surface slope $y' = \partial y / \partial x$. The key point of our approach is that the above degrees of freedom are assumed to be of dissipative type, so that, when they are not coupled, their relaxation to the steady state is governed by the Debye-type equations:

$$\frac{d\dot{x}}{dt} = -\frac{\dot{x}}{\tau_x}, \quad (3)$$

$$\frac{d\dot{y}}{dt} = -\frac{\dot{y}}{\tau_y^{(0)}}, \quad (4)$$

$$\frac{dy'}{dt} = \frac{y'_0 - y'}{\tau_S}, \quad (5)$$

where τ_x , $\tau_y^{(0)}$ and τ_S are the relaxation times of the velocity components and the slope, respectively. Eqs. (3) – (5) imply that the sand is at rest in the stationary state, $\dot{x} = \dot{y} = 0$ and the equilibrium slope $y' = y'_0 \neq 0$ plays the role of a control parameter.

Since the motion of sand grain along different directions is not independent, Eq. (3) should be changed by adding the term $f = \dot{y}/\gamma$ due to liquid friction force along the y -axis (γ being the kinetic coefficient). Then, we have

$$\tau_x \ddot{x} = -\dot{x} + a^{-1} \dot{y}, \quad (6)$$

where $a \equiv \gamma/\tau_x$. Note that, owing to the diffusion equation $\dot{y} = Dy''$ (D is the diffusion coefficient), the friction force appears to be driven by the curvature of the sand pile surface:

$$f = (D/\gamma)y''. \quad (7)$$

On the other hand, when $\ddot{x} = 0$ (stationary state), solution of Eq. (6) defines the tangent line $y = ax + \text{const}$, so that the friction force $f = \tau_x^{-1} \dot{x}$ is proportional to the horizontal component of the sand velocity. Taking into consideration the relation (7) and using the chain rule $dy'/dt = \dot{y}' + y''\dot{x}$, from Eq. (5) one obtains the equation of motion for the slope:

$$\tau_S \dot{y}' = (y'_0 - y') - (\tau_S/D) \dot{y} \dot{x}. \quad (8)$$

Following the same line, the equation for the vertical component of the velocity can be deduced

$$\tau_y \ddot{y} = -\dot{y} + \frac{\tau_y}{\tau_x} y' \dot{x}, \quad \frac{1}{\tau_y} \equiv \frac{1}{\tau_y^{(0)}} \left(1 + \frac{y'_0}{a} \frac{\tau_y^{(0)}}{\tau_x} \right). \quad (9)$$

Note the higher order terms are disregarded in Eq. (9) and the renormalized relaxation time τ_y depending on the stationary slope y'_0 is introduced.

Equations (6), (8), (9) obtained constitute the basis for self-consistent description of the sand flow on the surface with the slope y' driven by the control parameter y'_0 . The distinguishing feature of these equations is that nonlinear terms, that enter Eqs. (8), (9), are of opposite signs, while Eq. (6) is linear. Physically, the latter means that on the early stage the avalanche begins motion along the tangent $y = ax + \text{const}$. The negative sign of the last term in Eq. (8) can be regarded as a manifestation of Le Chatelier principle, i.e., since the slope increase results in the formation of an avalanche, the velocity components \dot{x} and \dot{y} tend to impede the growth of the slope. The positive feedback of \dot{x} and y' on \dot{y} in Eq. (9) plays a fundamental part in the problem. As we shall see later, it is precisely the reason behind the self-organization that brings about the avalanche generation.

After suitable rescaling, Eqs. (6), (8), (9) can be rewritten in the form of the well-known Lorenz system:

$$\dot{u} = -u + v, \quad (10)$$

$$\epsilon \dot{v} = -v + uS, \quad (11)$$

$$\delta \dot{S} = (S_0 - S) - uv, \quad (12)$$

where $u \equiv (\tau_y/\tau_x)^{1/2} (\tau_S/D)^{1/2} \dot{x}$, $v \equiv (\tau_y/\tau_x)^{1/2} (\tau_S/D)^{1/2} \dot{y}/a$ and $S \equiv (\tau_y/\tau_x) y'/a$ are the dimensionless velocity components and the slope, respectively; $\epsilon \equiv \tau_y/\tau_x$, $\delta \equiv \tau_S/\tau_x$ and the dot now stands for the derivative with respect to the dimensionless time t/τ_x . In the general case, the system (10)–(12) cannot be solved analytically, but in the simplest case, where $\epsilon \ll 1$ and $\delta \ll 1$, the vertical velocity v and the slope S can be eliminated by making use the adiabatic approximation that implies neglecting of the left hand side of Eqs. (11), (12). As a result, the dependencies of S and v on the horizontal velocity u are given by

$$S = \frac{S_0}{1 + u^2}, \quad v = \frac{S_0 u}{1 + u^2}. \quad (13)$$

Note that, under u is within the physically meaningful range between 0 and 1, the slope S is a monotonically decreasing function of u , whereas the velocity v increases with u (at $u > 1$ we have $dv/du < 0$ and the flow of the sand becomes unstable).

Substitution of the second Eq. (13) into Eq. (10) yields the Landau-Khalatnikov equation

$$\dot{u} = -\frac{\partial E}{\partial u} \quad (14)$$

with the kinetic energy

$$E = \frac{1}{2}u^2 - \frac{1}{2}S_0 \ln(1 + u^2). \quad (15)$$

For $S_0 < 1$, the u -dependence of E is monotonically increasing and the only stationary value of u equals zero, $u_0 = 0$, so that there are no avalanches in this case. Obviously, such steady-state relevant to absorbing configuration studied in Ref. [20]. If the slope S_0 exceeds the critical value, $S_c = 1$, the kinetic energy assumes the minimum with nonzero steady state velocity components $u_e = v_e = (S_0 - 1)^{1/2}$ and the slope $S_e = 1$.

The above scenario represents supercritical regime of the avalanche formation and addresses to the second-order phase transition [16]. The latter can be easily seen from the expansion of the kinetic energy (15) in power series of $u^2 \ll 1$. So the critical exponents γ, δ, ν are identical to those obtained within the framework of the mean-field theory [19]. However, the magnitude $\beta = 1/2$ is twice as little because our order parameter (being the velocity) is not reduced to the same (the number of active sites) in theory [19].

The drawback of the outlined approach is that it fails to account for the subcritical regime of the self-organization that is the reason for the appearance of avalanches and analogous to the first-order phase transition, rather than the second-order one. So one has to modify the above theory by assuming that the effective relaxation time $\tau_x(u)$ increases with velocity u from value $\tau_x(1 + m)^{-1}$, $m > 0$ to τ_x [17]. The simplest two-parameter approximation is

$$\frac{\tau_x}{\tau_x(u)} = 1 + \frac{m}{1 + (u/u_0)^2}, \quad (16)$$

where $0 < u_0 < 1$. The expression for the kinetic energy (15) then changes by adding the term

$$\Delta E = \frac{m}{2}u_0^2 \ln \left[1 + \left(\frac{u}{u_0} \right)^2 \right] \quad (17)$$

and the stationary values of u are following:

$$u_e^m = u_{00} \left\{ 1 \mp \left[1 + u_0^2 u_{00}^{-4} (S_0 - S_c) \right]^{1/2} \right\}^{1/2}, \quad (18)$$

$$2u_{00}^2 \equiv (S_0 - 1) + S_c u_0^2, \quad S_c \equiv 1 + m.$$

The upper sign in the right hand side of Eq. (18) meets the value of the unstable state u^m , where the kinetic energy $E + \Delta E$ has the maximum, the lower one corresponds to the stable state u_e . The corresponding value of the stationary slope

$$S^m = \frac{1 + u_{00}^2 + \sqrt{(1 + u_{00}^2)^2 - (1 - u_0^2) S_0}}{1 - u_0^2} \quad (19)$$

smoothly increases from the value

$$S_{\min} = 1 + u_0 \sqrt{m/(1 - u_0^2)} \quad (20)$$

at the parameter $S_0 = S_{c0}$ with

$$S_{c0} = (1 - u_0^2) S_{\min}^2 \quad (21)$$

to the marginal value $S_c = 1 + m$ at $S_0 = S_c$. The S_0 -dependencies of u_e , u_m , and S_e are presented in Fig. 1. As is shown in Fig. 1a, under the adiabatic condition $\tau_S \ll \tau_x$ is met and the parameter S_0 slowly increases being below S_c ($S_0 \leq S_c$), no avalanches can form. At the point $S_0 = S_c$ the velocity u_e jumps upward to the value $\sqrt{2}u_{00}$ and its further smooth increase is determined by Eq. (18). If the parameter S_0 then goes downward the velocity u_e continuously decreases to the point, where $S_0 = S_{c0}$ and $u_e = u_{00}$. At this point the velocity jump-like goes down to zero. Referring to Fig. 1b, the stationary slope S_e shows a linear increase from 0 to S_c with the parameter S_0 being in the same interval and, after the jump down to the value $(1 - u_0^2)^{-1}$ at $S_0 = S_c$, S_e smoothly decays to 1 at $S_0 \gg S_c$. Under the parameter S_0 then decreases from S_c down to S_{c0} , the slope grows. When the point (21) is reached, the avalanche stops, so that the slope undergoes the jump from the value (20) up to the one defined by Eq. (21). For $S_0 < S_{c0}$ again the parameter S_e does not differ from S_0 . Note that this subcritical regime is realized provided the parameter m , that enters the dispersion law (16), is greater than

$$m_{\min} = \frac{u_0^2}{1 - u_0^2}. \quad (22)$$

Clearly, according to the picture described, the avalanche generation is characterized by the well pronounced hysteresis, when the grains of sand initially being at rest begin to move downhill only if the slope of the surface exceeds its limiting value $S_c = 1 + m$, whereas the slope S_{c0} needed to stop the avalanche is less than S_c (see Eqs. (20), (21)). This is the case in the limit $\tau_S/\tau_x \rightarrow 0$ and the hysteresis loop shrinks with the growth of the adiabaticity parameter $\delta \equiv \tau_S/\tau_x$. In addition to the smallness of δ , the adiabatic approximation implies the ratio $\tau_y/\tau_x \equiv \epsilon$ is also small. In contrast to the former, the latter does not seem to be realistic for the system under consideration, where, in general, $\tau_y \approx \tau_x$. Thus, it is of interest to study to what extent the finite value of ϵ could change the results.

Owing to the condition $\delta \ll 1$, Eq. (12) is still algebraic and S can be expressed in terms of u and v . As a result, we derive the system of two nonlinear differential equations that can be studied by the phase portrait method [17]. The phase portraits for various values of ϵ are displayed in Fig. 2, where the node point O represents the stationary state and the saddle point S is related to the maximum of the kinetic energy. As is seen from the figure, independently of ϵ , there is the universal section that attracts all phase trajectories and its structure is appeared to be almost insensitive to changes in ϵ . Analysis of time dependencies $v(t)$ and $u(t)$ reveals that the velocity components slow down appreciably on this section in comparison to the rest parts of trajectories that are almost rectilinear (it is not difficult to see that this effect is caused by the smallness of the parameter δ). Since the most of time the system is in vicinity of this universal section, we arrive at the conclusion that finite values of ϵ do not affect qualitatively the above results obtained in the adiabatic approximation.

III. NOISE INFLUENCE ON AVALANCHE FORMATION

We focus now on studying the affect of additive noises of the velocity components u , v , and the slope S . With this aim, we should add to right hand parts of Eqs. (10) – (12) the stochastic terms $I_u^{1/2}\xi$, $I_v^{1/2}\xi$, $I_S^{1/2}\xi$, respectively [here the noise intensities I_u , I_v , I_S are

measured in units $(\tau_x/\tau_y)(D/\tau_S)$, $a^2(\tau_x/\tau_y)(D/\tau_S)$, $a^2(\tau_x/\tau_y)$, correspondingly, and $\xi(t)$ is δ -correlated stochastic function] [26]. Then, within the adiabatic approximation, equations (11), (12) could be reduced to the time-dependencies

$$v(t) = \bar{v} + \tilde{v}\xi(t), \quad S(t) = \bar{S} + \tilde{S}\xi(t); \quad (23)$$

$$\begin{aligned} \bar{v} &\equiv S_0 u d(u), & \tilde{v} &\equiv \sqrt{I_v + I_S u^2} d(u), \\ \bar{S} &\equiv S_0 d(u), & \tilde{S} &\equiv \sqrt{I_S + I_v u^2} d(u), & d(u) &\equiv (1 + u^2)^{-1}. \end{aligned} \quad (24)$$

Here deterministic components are reduced to Eqs. (13), whereas fluctuational ones follow from the known property of additivity of variances of independent Gaussian random quantities [26]. Thus, using slaving principle inherent in synergetics [27] transforms noises of both vertical velocity component v and slope S , having been adiabatic initially, to multiplicative form. As a result, combination of Eqs. (10), (23), (24) arrives at Langevin equation

$$\dot{u} = f(u) + \sqrt{I(u)} \xi(t), \quad f \equiv -\frac{\partial E}{\partial u}, \quad (25)$$

where force f is related to the energy E determined by Eq. (15) and expression for effective noise intensity

$$I(u) \equiv I_u + (I_v + I_S u^2) d^2(u) \quad (26)$$

is obtained in accordance with above mentioned property of noise variances additivity. In order to avoid mistakes, one should notice that direct insertion of Eqs. (23), (24) into (10) results in appearance of stochastic addition

$$\left[I_u^{1/2} + (I_v^{1/2} + I_S^{1/2} u) d(u) \right] \xi(t), \quad (27)$$

whose squared amplitude is quite different from effective noise intensity (26). Moreover, contrary to expressions (24), direct using adiabatic approximation in Eqs. (11), (12) reduces fluctuational additions in Eqs. (23) to the forms: $\tilde{v} \equiv (I_v^{1/2} + I_S^{1/2} u) d(u)$, $\tilde{S} \equiv (I_S^{1/2} - I_v^{1/2} u) d(u)$. The latter is obviously erroneous since the effective noise of the slope \tilde{S} disappears entirely for the horizontal velocity $u = \sqrt{I_S/I_v}$. The reason of such contradiction is that Langevin equation, being stochastic in nature, does not permit usage of usual analysis methods (see [26]).

To continue along standard direction, let us write the Fokker-Planck equation related to Langevin equation (25):

$$\frac{\partial P(u, t)}{\partial t} = \frac{\partial}{\partial u} \left\{ -f(u) P(u, t) + \frac{\partial}{\partial u} [I(u) P(u, t)] \right\}. \quad (28)$$

At steady state, which will be considered only, the probability distribution $P(u, t)$ becomes time-independent function $P(u)$ and usual condition, that expression in braces of right hand part in Eq. (28) is zero, arrives at stationary distribution

$$P(u) = Z^{-1} \exp\{-U(u)\}, \quad (29)$$

where Z is a normalization constant and effective energy

$$U(u) = \ln I(u) - \int_0^u \frac{f(u')}{I(u')} du', \quad f \equiv -\frac{\partial E}{\partial u}, \quad (30)$$

is determined by the bare energy E , Eq. (15) and the noise intensity $I(u)$, Eq. (26) [28]. Combining these expressions, we might find the explicit form of $U(u)$, which is too cumbersome to be reproduced here. The equation which defines the locations of the maxima of distribution function $P(u)$

$$x^3 - S_0 x^2 - 2I_S x + 4(I_S - I_v) = 0, \quad x \equiv 1 + u^2, \quad (31)$$

is much simpler. According to Eq. (31), they are insensitive to changes in the intensity of noise I_u of the velocity component u , but are determined by the value S_0 of the sand pile slope and the intensities I_v , I_S of the noises of vertical velocity component v and slope S , which acquire the multiplicative character in Eq. (26). Hence, it can be put for simplicity $I_u = 0$ and Eqs. (15), (30), (26) give the following expression for the effective energy:

$$U(u) = \frac{1}{2} \left[\frac{u^4}{2} + (2 - S_0 - i)u^2 + (1 - i)(1 - S_0 - i) \ln(i + u^2) \right] + I_S \ln[g_S^2(u) + ig_v^2(u)], \quad i \equiv I_v/I_S. \quad (32)$$

According to Eq. (31), the effective energy (32) has a minimum at $u = 0$ if the driven slope S_0 does not exceed the critical level

$$S_c = 1 + 2I_S - 4I_v, \quad (33)$$

whose value increases at increasing intensity of noise of the sand pile slope, but decreases with one of the vertical velocity. Here, sand grains are at rest. In the simple case $I_v = 0$, the avalanche creation is related to solutions

$$u_{\pm}^2 = \frac{1}{2} \left[S_0 - 3 + \sqrt{(3 - S_0)^2 + 4(2S_0 - 3 + 2I_S)} \right], \quad (34)$$

which are obtained from Eq. (31) after elimination of the root $u^2 = 0$. The magnitude of this solution has its minimum

$$u_c^2 = \frac{1}{2} \left[(S_0 - 3) - \sqrt{(S_0 + 7)(S_0 - 1)} \right] \quad (35)$$

on the line defined by expression (33) with $I_v = 0$. At $S_0 < 4/3$ the roots $\pm u_c$ are complex, at $S_0 = 4/3$ they become zero, at $S_0 > 4/3$ they are real and $u_+ = -u_-$. In this way, the tricritical point

$$S_0 = 4/3, \quad I_S = 1/6 \quad (36)$$

addresses to the appearance of roots $u_{\pm} \neq 0$ of Eq. (31) (avalanche creation). If condition (33) is satisfied, the root $u = 0$ corresponds to the minimum of the effective energy (32) at

$S_0 < 4/3$, whereas at $S_0 > 4/3$ this root corresponds to the maximum, and the roots u_{\pm} – to symmetrical minima.

Now, we find another condition of stability of roots u_{\pm} . Setting the discriminant of Eq. (31) equal to zero, we get the equations

$$I_S = 0, \quad I_S^2 - I_S \left[\frac{27}{2} \left(1 - \frac{S_0}{3} \right) - \frac{S_0^2}{8} \right] + \frac{S_0^3}{2} = 0, \quad (37)$$

the second of which gives

$$2I_S = \left[\frac{27}{2} \left(1 - \frac{S_0}{3} \right) - \frac{S_0^2}{8} \right] \pm \left\{ \left[\frac{27}{2} \left(1 - \frac{S_0}{3} \right) - \frac{S_0^2}{8} \right]^2 - 2S_0^3 \right\}^{1/2}. \quad (38)$$

This equation defines a bell-shaped curve $S_0(I_S)$, which intersects the horizontal axis at the points $I_S = 0$ and $I_S = 27/2$, and has a maximum at

$$S_0 = 2, \quad I_S = 2. \quad (39)$$

It is easy to see that for $I_v = 0$ this line touches the curve (33) at point (36).

Let us consider now the more general case of two multiplicative noises $I_v, I_S \neq 0$. Introducing the parameter $a = 1 - i$, $i \equiv I_v/I_S$ and the renormalized variables $\tilde{I} \equiv I_S/a^2$, $\tilde{S}_0 \equiv S_0/a$, $\tilde{u}^2 = (1 + u^2)/a - 1$, at $i < 1$ we reproduce all above expressions with the generalized energy \tilde{U}/\tilde{I} in Eq. (32). Thus, action of the noise of the vertical velocity component v is reduced to the renormalization of the extremum value of the horizontal one by the quantity $(a^{-1} - 1)^{1/2}$. As a result, the region of divergence $\tilde{u} \approx 0$ becomes inaccessible.

The condition of extremum of the generalized energy (32) splits into two equations, one of which is simply $u = 0$, and the other is given by Eq. (31). As mentioned above, analysis of the latter indicates that the line of existence of the zero solution is defined by expression (33). The tricritical point has the coordinates

$$S_0 = \frac{4}{3}(1 - I_v), \quad I_S = \frac{1}{6}(1 + 8I_v). \quad (40)$$

The phase diagram for the fixed intensities I_v is shown in Fig. 3. Here the curves 1, 2 define the thresholds of absolute loss of stability for the fluxless and flux steady-states, respectively. Above line 1 the system occurs in a stable flux state, below curve 2 it is in fluxless one, and between these lines the two-phase domain is realized. For $I_v < 1/4$ situation is generally the same as in the simple case $I_v = 0$ (see Fig. 3a). At $I_v > 1/4$ the avalanches formation is possible even for small intensities I_S of the slope noise (Fig. 3b). According to (40), the tricritical point occurs on the I_S -axis at $I_v = 1$, and for the noise intensity I_v larger than the critical value $I_v = 2$ the stable fluxless state disappears (see Fig. 3c).

The above consideration shows that the dissipative dynamic of grains flow in a real sand pile can be represented within the framework of the Lorenz model, where the horizontal and vertical velocity components play roles of the order parameter and its conjugate field, respectively, and the sand pile slope is the control parameter. In Section II, the noiseless case is examined to show that an avalanche is created if the externally driven sand pile slope y'_0 is larger than the critical magnitude

$$y'_c = (\tau_x \tau_y)^{-1/2} \gamma. \quad (41)$$

In this sense, the systems with small values of the kinetic coefficient γ and large relaxation times τ_x, τ_y of the velocity components are preferred. However, the sand flow appears here as a phase transition because the avalanche creation in the noiseless case is possible only due to the externally driven growth of the sand pile slope.

Accounting the additive noises of the above degrees of freedom shows that the stochasticity influence is non-essential for the horizontal velocity component and is crucial for both the vertical one and the sand pile slope. The avalanche appears spontaneously if the dimensionless noise intensities are connected by linear relation

$$I_S = -\frac{1}{2} + 2I_v, \quad (42)$$

following from Eq. (31) at conditions $x = 1$ ($u = 0$), $S_0 = 0$. According to Eq. (42), in absence of the sand pile slope noise the avalanche is created if the intensity of vertical velocity component exceeds the value

$$I_{v0} = \frac{1}{4} \frac{D\gamma^2}{\tau_x \tau_y \tau_S}, \quad (43)$$

corresponding to the point O in Fig. 4. Increase of both the vertical velocity and the sand pile slope noises causes avalanche formation if its intensities are bounded by the condition (42). With further increase of these intensities above magnitudes

$$I_{v1} = \frac{D\gamma^2}{\tau_x \tau_y \tau_S}, \quad I_{S1} = \frac{3}{2} \frac{\gamma^2}{\tau_x \tau_y}, \quad (44)$$

the domain of the mixed state appears at the point T in Fig. 4. If the noise intensity of the vertical velocity is more than the larger value

$$I_{v2} = 2 \frac{D\gamma^2}{\tau_x \tau_y \tau_S}, \quad (45)$$

corresponding to the sand pile slope noise $I_{S2} = 6\gamma^2/\tau_x \tau_y$ (the point C in Fig. 4), the fluxless steady-state disappears at all.

Physically, we have to take into consideration that the SOC regime is not relevant to flux-type avalanche state itself, but rather to an intermittent regime of avalanche formation corresponding to the domains on the phase diagrams in Figs. 3, 4, where a mixture of both phases A and N (avalanche and non-avalanche) exists. According to above analysis, such an intermittent behavior may be realized within the region located upper the line (42) and outside the curve determined by the equation

$$I_v = I_S \left[1 - \left(\frac{2}{27} \right)^{1/2} \sqrt{I_S} \right] \quad (46)$$

for the dimensionless values I_v, I_S . Corresponding phase diagram is depicted in Fig. 4 to show very non-trivial form (especially, within the domain $I_{v1} \leq I_v \leq I_{v2}$).

IV. GENERALIZING SELF-SIMILARITY

To proceed the consideration of the system behavior, let us examine explicit form of the probability (29) determined for different regimes by the effective energy (30). In the case $I_u, I_S \ll I_v$, we obtain Gibbs-type distribution

$$P(u) \approx I_v^{-1}(1+u^2)^2 \exp \left\{ I_v^{-1} \int f(u)(1+u^2)^2 du \right\}, \quad f(u) \equiv -u + S_0 u / (1+u^2), \quad (47)$$

being opposite to the power dependence inherent in self-similar systems. Contrary, at intermittent behavior, when $I_u, I_v \ll I_S$, supercritical values of the slope noise intensity I_S cause the following distribution form:

$$P(u) \approx I_S^{-1} \left(\frac{1+u^2}{u} \right)^2 \exp \left\{ I_S^{-1} \int \frac{f(u)(1+u^2)^2}{u^2} du \right\} \sim u^{-2}. \quad (48)$$

Thus, the case $I_u, I_v \ll I_S$ addresses to the power-law distribution being relevant to self-similar behavior. However, as corresponding consideration [28] shows, obtained exponent is not reduced to integer 2, generally.

To get rid off such a restriction, the multiplier u in nonlinear terms of Eqs. (10) – (12) is supposed to be replaced by u^a , where an exponent $0 \leq a \leq 1$. With accounting the stochastic additions one obtains then the basic equations in dimensionless form

$$\begin{aligned} \dot{u} &= -u + v + \sqrt{I_u} \xi(t), \\ \epsilon \dot{v} &= -v + u^a S + \sqrt{I_v} \xi(t), \\ \delta \dot{S} &= (S_0 - S) - u^a v + \sqrt{I_S} \xi(t). \end{aligned} \quad (49)$$

Thus, it is appeared that the agreement of the Lorenz self-organization scheme with SOC conception related to self-similar systems is achieved if one assumes that both positive and negative feedbacks are fractional in the nature. Within such a supposition, the adiabatic approximation $\epsilon, \delta \ll 1$ arrives at the Langevin equation (cf. Eq. (25))

$$\dot{u} = f_a(u) + \sqrt{I_a(u)} \xi(t), \quad (50)$$

where force $f_a(u)$ and noise intensity $I_a(u)$ are as follows:

$$\begin{aligned} f_a(u) &\equiv -u + S_0 u^a d_a(u), \\ I_a(u) &\equiv I_u + (I_v + I_S u^{2a}) d_a^2(u), \quad d_a(u) \equiv (1 + u^{2a})^{-1}. \end{aligned} \quad (51)$$

Corresponding distribution (cf. Eqs. (29), (30))

$$P_a(u) = \frac{Z^{-1}}{I_a(u)} \exp \{-E_a(u)\} \quad (52)$$

with partition function Z is determined by effective potential

$$E_a(u) \equiv - \int_0^u \frac{f_a(u')}{I_a(u')} du'. \quad (53)$$

Extremum points of this distribution are determined by equation

$$2aI_S u^{2a} + (1 + u^{2a})^2 u^{1-a} [S_0 - u^{1-a} (1 + u^{2a})] = 2a(I_S - 2I_v), \quad (54)$$

which gives the boundary of the flux state

$$I_S = 2I_v, \quad (55)$$

related to $u = 0$. Critical values of state parameters are fixed by condition $|\frac{du}{dS_0}| = \infty$ to arrive at additional equation

$$u^{2(1-a)} (1 + u^{2a})^2 [(2 + a^{-1}) + (a^{-1} - 1) u^{-2a}] - \frac{1}{2} S_0 u^{1-a} (1 + u^{2a}) [(3 + a^{-1}) + (a^{-1} - 1) u^{-2a}] = 2aI_S. \quad (56)$$

Expressions (54) – (56) generalize the simple equalities (31), (42) and (46) related to the case $a = 1$.

Above expressions show that qualitative results of Section III obtained for the particular case $a = 1$ are kept invariant at passage to general case $0 \leq a \leq 1$. Indeed, the most essential difference is observed for noiseless case, namely the steady-state velocity u becomes nonzero within whole interval of the driven slope S_0 (see Fig. 5). Increase of the vertical velocity noise I_v causes monotonic u -growth, whereas I_S -increase arrives at an effective barrier formation near the point $u = 0$, so that the dependence $u(S_0)$ becomes non-monotonic in character at magnitudes I_S above the straight line (55) (see Figs. 6). Here, by analogy with noiseless case (see Fig. 1), lower branches of curves correspond to unstable magnitudes of the order parameter, the uppers – to stable ones. According to Fig. 7, the domain, where avalanches can not be created, is located near an intermediate magnitudes of the state parameters S_0 , I_v , I_S . The phase diagram related to the avalanche formation reveals the same form as for the simplest case $a = 1$, but the straight line (42) shifts abruptly to (55) with escaping the point $a = 1$ (compare Fig. 8 with Fig. 4). According to Fig. 9, increase of the vertical velocity noise I_v increases the domain of the avalanche formation.

V. SIZE DISTRIBUTION IN SELF-SIMILAR ENSEMBLE OF AVALANCHES

Contrary to the previous, when the process of a single avalanche formation has been considered, further we aim to study analytically self-similar size distribution (2) over avalanche ensemble. This means that, along line of Section III, we will account for noises of complete set of freedom degrees, on the one hand, and the fractional feedback type of introduced in Section IV, on the other one. Thereby, the Lorenz system unified in above manner is the basis of our examination. However, instead of visible geometric-and-mechanic characteristics of 'real' sand pile, the system under consideration is parametrized now by a set of pseudo-thermodynamical values, which describes the avalanche ensemble in a spirit of the famous Edwards paradigm [22], [23] generalized to nonstationary system. In this line, we study time dependencies of the avalanche size, nonextensive complexity and nonconserved energy of the moving grains. Within the framework of usual synergetic approach, these degrees of freedom play roles of order parameter, conjugate field and control parameter, respectively.

It is very important that using slaving principle of synergetics and fractional nature of the system feedback are shown above to stipulate multiplicative character of noise. It will be appeared below, this causes a nonextensivity of applied thermodynamical scheme, so that we have to use q -weighted averages instead of usual ones. So, energy of moving sand grains is defined by expression

$$\zeta_q \equiv \sum_i \zeta_i p_i^q, \quad (57)$$

where p_i is a probability to move grain i with energy ζ_i , $q \neq 1$ is a positive parameter being measure of the system nonextensivity determined below. Respectively, nonextensive complexity of moving sand grains is an analog of Tsallis entropy [24] to be determined as follows:

$$\Sigma_q \equiv -\frac{\sum_i p_i^q - 1}{q - 1}. \quad (58)$$

Three-parameter set of standard synergetic scheme [27] is completed by avalanche size s .

Following above elaborated line, we postulate that self-consistent behavior of the system under consideration is presented adequately by set of above quantities governed by the Lorenz-type equations (cf. Eqs. (49))

$$\begin{aligned} \tau_s \dot{s} &= -s + a_s \Sigma_q + \sqrt{I_s} \xi(t), \\ \tau_\Sigma \dot{\Sigma}_q &= -\Sigma_q + a_\Sigma s^{\tau/2} \zeta_q + \sqrt{I_\Sigma} \xi(t), \\ \tau_\zeta \dot{\zeta}_q &= (\zeta^0 - \zeta_q) - a_\zeta s^{\tau/2} \Sigma_q + \sqrt{I_\zeta} \xi(t). \end{aligned} \quad (59)$$

Here $\tau_s, \tau_\Sigma, \tau_\zeta$ note relaxation times of corresponding values, a_s, a_Σ, a_ζ are related feedback parameters, I_s, I_Σ, I_ζ are respective noise intensities, τ is a positive exponent and ζ^0 is externally driven energy of sand motion. The distinguishing feature of the first of these equations is that in noiseless case genuine characteristics s, Σ_q are connected in linear manner. On the other hand, connection of thermodynamic-type values ζ_q, Σ_q with the avalanche size s is stated by two last equations (59) to be nonlinear in nature. Physically, this means linear relation between complexity and avalanche size near steady-states. Running away these derives to negative feedback of the avalanche size with the complexity that arrives at the energy decrease – in accordance with Le Chatelier principle, and positive feedback between the avalanche size and the energy that brings the complexity increase to be reason of the avalanche ensemble self-organization.

To analyze the system (59), it is convenient to measure the time t in unit τ_s , as well as the values s, Σ_q, ζ_q and I_s, I_Σ, I_ζ are related to the scales:

$$\begin{aligned} s^{sc} &\equiv (a_\Sigma a_\zeta)^{-\frac{1}{\tau}}, \quad \Sigma_q^{sc} \equiv a_s^{-1} (a_\Sigma a_\zeta)^{-\frac{1}{\tau}}, \quad \zeta_q^{sc} \equiv a_s^{-1} a_\Sigma^{-\left(\frac{1}{\tau} + \frac{1}{2}\right)} a_\zeta^{-\left(\frac{1}{\tau} - \frac{1}{2}\right)}, \\ I_s^{sc} &\equiv (a_\Sigma a_\zeta)^{-\frac{2}{\tau}}, \quad I_\Sigma^{sc} \equiv a_s^{-2} (a_\Sigma a_\zeta)^{-\frac{2}{\tau}}, \quad I_\zeta^{sc} \equiv a_s^{-2} a_\Sigma^{-\left(\frac{2}{\tau} + 1\right)} a_\zeta^{-\left(\frac{2}{\tau} - 1\right)}. \end{aligned} \quad (60)$$

Then, the modified Lorenz system (59) takes the simple form

$$\begin{aligned} \dot{s} &= -s + \Sigma_q + \sqrt{I_s} \xi(t), \\ \vartheta \dot{\Sigma}_q &= -\Sigma_q + s^{\tau/2} \zeta_q + \sqrt{I_\Sigma} \xi(t), \\ \theta \dot{\zeta}_q &= (\zeta^0 - \zeta_q) - s^{\tau/2} \Sigma_q + \sqrt{I_\zeta} \xi(t), \end{aligned} \quad (61)$$

where relaxation time ratios are introduced:

$$\vartheta \equiv \tau_\Sigma/\tau_s, \quad \theta \equiv \tau_\zeta/\tau_s. \quad (62)$$

It is worthwhile to notice that system (61) is passed to the form of Eqs. (49) if the values s , Σ_q , ζ_q , $\tau/2$, ϑ , θ are replaced by u , v , S , a , ϵ , δ , respectively.

It is well-known that complete set of SOC systems can be reduced to one of two families [19]: systems with deterministic dynamics extremely driven by random environment (growing interface models, Bak-Sneppen evolution model and so one) and the stochastic dynamics family (models of earthquakes, forest-fire et cetera).¹ Remarkable peculiarity of obtained system (61) is a possibility to present in natural manner both mentioned families. So, the former is related to noiseless case, when $I_s, I_\Sigma, I_\zeta = 0$ but magnitude of the energy relaxation time is above than the ones for complexity and avalanche size ($\tau_\zeta \geq \tau_\Sigma, \tau_s$); on the other hand, a parameter of environment drive ζ^0 has to take magnitudes above the critical one $\zeta_c = 1$ [17]. In such a case, the system (61) describes strange attractor [27] that may represent behavior of the first type SOC systems. Proper stochastic behavior is relevant to nonzerorth noise intensities $I_s, I_\Sigma, I_\zeta \neq 0$ that make possible the SOC regime appearance even in absence of driven affect ($\zeta^0 = 0$).

Taking into account that problem of Lorenz strange attractor is well known [27], we will restrict ourselves further with treatment of the stochastic system, where the adiabatic conditions $\vartheta, \theta \ll 1$ are applicable. Then, two last equations of the system (61) arrive at dependencies type of Eqs. (23)

$$\Sigma_q(t) = \bar{\Sigma}_q + \tilde{\Sigma}_q \xi(t), \quad \zeta_q(t) = \bar{\zeta}_q + \tilde{\zeta}_q \xi(t), \quad (63)$$

where deterministic and fluctuational components are determined as follows (cf. Eqs. (24))

$$\begin{aligned} \bar{\Sigma}_q &\equiv \zeta^0 s^{\tau/2} d_\tau(s), & \tilde{\Sigma}_q &\equiv \sqrt{I_\Sigma + I_\zeta s^\tau} d_\tau(s); \\ \bar{\zeta}_q &\equiv \zeta^0 d_\tau(s), & \tilde{\zeta}_q &\equiv \sqrt{I_\zeta + I_\Sigma s^\tau} d_\tau(s), & d_\tau(s) &\equiv (1 + s^\tau)^{-1}. \end{aligned} \quad (64)$$

So, due to the slaving principle of synergetics, initially adiabatic noises of the complexity and energy are transformed to multiplicative form. On the other hand, relation between the complexity and energy

$$\bar{\Sigma}_q = \sqrt{\bar{\zeta}_q(\zeta^0 - \bar{\zeta}_q)}, \quad (65)$$

following from the dependencies (64), arrives at expression

$$T = - \left(1 - \frac{\zeta^0}{2\bar{\zeta}_q} \right)^{-1} \sqrt{\frac{\zeta^0}{\bar{\zeta}_q} - 1} \quad (66)$$

for effective temperature $T \equiv \partial \bar{\zeta}_q / \partial \bar{\Sigma}_q$. As is depicted in Fig. 10a, so defined temperature increases monotonically with energy growth from magnitude $T = 0$ at $\bar{\zeta}_q = 0$ to infinity

¹Generally, we face here with much more complicated problem, see Ref. [31].

at the point $\bar{\zeta}_q = \zeta^0/2$. Here, the temperature T breaks abruptly to negative infinity and then increases monotonically again to initial magnitude $T = 0$ at $\bar{\zeta}_q = \zeta^0$. This means that inside domain $0 \leq \bar{\zeta}_q < \zeta^0/2$ the avalanche system is dissipative to behave in usual manner; contrary, within domain $\zeta^0/2 < \bar{\zeta}_q \leq \zeta^0$ self-organization process evolves, so that an energy increase derives to complexity decrease, in accordance with negative value of temperature. At steady state, where avalanche has stationary size $s_0 = \sqrt{\zeta^0 - 1}$, the temperature takes the stationary magnitude

$$T_0 = -\frac{\sqrt{\zeta^0 - 1}}{1 - \zeta^0/2} \quad (67)$$

being negative within supercritical domain $1 \leq \zeta^0 < 2$. According to Fig. 10b, the stationary temperature T_0 decreases monotonically with the driven energy from the zeroth magnitude at $\zeta^0 = 1$ to negative infinity at $\zeta^0 = 2$.

Presented self-organization regime addresses to externally driven systems, which are relevant to the usual phase transition but not to the SOC itself. To study the latter within above consideration, let us combine Eqs. (63), (64) with the first of equations (61) along the line, which has been used above for obtaining Langevin equation (25). So, by analogy with Section IV, we arrive at stochastic equation (50), where effective force and noise intensity are given by Eqs. (51) with accuracy to the replacements mentioned after Eqs. (62): the quantities $s, \Sigma_q, \zeta_q, \tau/2$ have to be taken instead of u, v, S, a . Then, all results obtained in Section IV can be used immediately. Particularly, it is appeared that influence of random scattering of avalanche size is non-essential, whereas energy and complexity noises affect crucially. Related picture is reflected by Fig. 8 taken in plane $I_\zeta - I_\Sigma$ formed by corresponding noise intensities of avalanche ensemble. By this, mixed domain A+N respected to intermittency regime is bounded by the straight line (55) and bell-shaped curve type of Eqs. (46). According to Fig. 9, where exponent a has to be replaced by $\tau/2$, random scattering growth of the complexity extends the SOC domain along axis of exponents τ .

We are in position now to consider the avalanche size distribution on the basis of equations (51) – (53). At arbitrary relations of noise intensities, general expressions are as follows:

$$\begin{aligned} P(s) &= \frac{Z^{-1}}{I(s)} \exp \left\{ \int_0^s \frac{f(s')}{I(s')} ds' \right\}; \\ f(s) &\equiv -s + \zeta^0 s^{\tau/2} d_\tau(s), \\ I(s) &\equiv I_s + (I_\Sigma + I_\zeta s^\tau) d_\tau^2(s), \quad d_\tau(s) \equiv (1 + s^\tau)^{-1}. \end{aligned} \quad (68)$$

At SOC regime, the driven energy $\zeta^0 = 0$ and the distribution (68) behaves as depicted in Fig. 11 for different noise intensities of both energy and complexity. It is seen that the power-law dependence inherent in SOC regime is observed only within limits $s \ll 1$ and $I_s, I_\Sigma \ll I_\zeta$ (at condition $\zeta^0 = 0$). Here, the distribution (68) is reduced to the canonical form (2), where second multiplier takes the form

$$\mathcal{P}(s) = \frac{d_\tau^{-2}(s)}{Z} \exp \left\{ -I_\zeta^{-1} \int_0^s \frac{d_\tau^{-2}(s')}{(s')^{\tau-1}} ds' \right\}, \quad d_\tau(s) \equiv (1 + s^\tau)^{-1}. \quad (69)$$

It is easily to see that deviation of this multiplier off a constant value is estimated with term $\sim s^{2-\tau}$, whose contribution increases remarkably with τ -decrease and growth of avalanche size to extremely large magnitudes $s \sim 1$, i. e., with escaping SOC domain. This confirmed by Fig. 12, where deviation $\delta\tau$ of the slope of dependence $P(s)$, Eqs. (68) within linear domain from the theory parameter τ is depicted as function of the parameter τ itself. It is seen, in accordance with above estimation, that the deviation $\delta\tau$ takes maximal value $\delta\tau < 10^{-1}\tau$ at non-essential magnitudes $\tau < 1$ or with noise intensity growth to enormous values $I_S \sim 10^3$.

VI. DISCUSSION

Remarkable peculiarity of expression (69) is that, within limits $s \ll 1$, $I_s, I_\Sigma \ll I_\zeta$ inherent in SOC regime, it can be rewritten in the form

$$\mathcal{P}(s) = \frac{d_\tau^{-2}(s)}{Z} \exp \left\{ - \frac{\Gamma(2-\tau)}{I_\zeta} \mathcal{I}_{-s}^{2-\tau} d_\tau^{-2}(s) \right\} \quad (70)$$

expressed in terms of standard Gamma-function $\Gamma(x)$ and fractional integral $\mathcal{I}_{-s}^{2-\tau}$ of order $2-\tau$, whose definition (A.1) is given in Appendix (for details, see Refs. [30], [31]). On the other hand, it is well-known [25] that such type expressions appear as a solution of fractional Fokker-Planck equation

$$\mathcal{D}_t^\omega \mathcal{P}(s, t) = \mathcal{D}_{-s}^\varpi \left\{ s \mathcal{P}(s, t) + \frac{I_\zeta}{\Gamma(\varpi)} \mathcal{D}_{-s}^\varpi [d_\tau^2 \mathcal{P}(s, t)] \right\}, \quad (71)$$

where fractional derivative \mathcal{D}_x^ϖ defined by Eq. (A.2) is used to be inverted to the fractional integral (A.1). Multiplying equation (71) by term $s^{2\varpi}$, for a α -average

$$|s| \equiv \langle s^\alpha \rangle^{\frac{1}{\alpha}}, \quad \langle s^\alpha \rangle \equiv \int_{-\infty}^{\infty} s^\alpha \mathcal{P}(s, t) ds, \quad \alpha > 0 \quad (72)$$

one obtains at $\alpha \equiv 2\varpi$

$$|s|^z \sim t, \quad z = \frac{2\varpi}{\omega}, \quad (73)$$

where z is dynamical exponent. This relation corresponds to large time limit, where only diffusional contribution is essential. Combining expressions (70), (73) and (A.1) arrives at relations $2-\tau = \varpi = z\omega/2$, which yields

$$\tau = 2 - \frac{z\omega}{2}. \quad (74)$$

Comparing this equation with the second of known relations (1), one obtains

$$\omega z = \frac{4}{D}. \quad (75)$$

Then, mean-field magnitudes $\omega = 1$ and $D = 4$ are related to dynamical exponent $z = 1$ that, in accordance with definition (73), addresses to unusual ballistic limit of SOC regime.

On the other hand, the fractional Fokker-Planck equation (71) arrives at usual diffusional regime with $z = 2$ only in artificial case, when time-derivative exponent is supposed to be $\omega = 1/2$.

Obvious reason for such discrepancy is non-consistent application of usual field relations (1) to Lorenz system (61). In this system, the role of different space directions is played by stochastic degrees of freedom s , Σ_q and ζ_q , whose number is $n = 3$. However, stochastic process evolves for every of these variables in plane spanned by given variable itself and conjugated momentum. Moreover, multiplicative character of noise, which is determined by exponent a in expressions (51), reduces fractal dimension of every plane to the value $2(1 - a)$ [28]. Thus, resulting fractal dimension of phase space, where stochastic system evolves, is as follows:

$$D = 2n(1 - a), \quad (76)$$

where one has $n = 3$ for used Lorenz system. Insertion of this dimension into expression (75) arrives at the connection $\omega z = 2$, which in contrast to above obtained relation $\omega z = 1$ is correct in the simplest case $\omega = 1$, $z = 2$ [the latter is relevant to single stochastic freedom degree ($n = 1$) with additive noise ($a = 0$)]. In general case, equations (74) – (76) yield final result

$$\tau = 2 \left[1 - \frac{1}{2n(1 - a)} \right]. \quad (77)$$

Respective dependencies are depicted in Figs.13a,b to show that exponent τ increases monotonically from minimum magnitude $\tau = 1$ at critical number $(1 - a)^{-1}$ to upper value $\tau = 2$ in limit $n \rightarrow \infty$; thereby, a -growth shifts dependence $\tau(n)$ to large magnitudes n , i. e., decreases exponent τ .

It is easily to see that relation (77) reproduces known results of different approaches for dimension D (see Ref. [32]). In the case related to mean-field theory, one has $\tau = 3/2$ and equation (77) expresses number of self-consistent stochastic equations being in need of treating SOC behavior as function of exponent of the corresponding multiplicative noise:

$$n = \frac{2}{1 - a}. \quad (78)$$

Thus, in accordance with Fig. 13c, self-consistent mean-field treatment becomes possible if the number of relevant equations is more than minimum magnitude $n_c = 2$. Approaches [5] – [7], [16], [19] represent examples of such considerations, where noise is supposed to be additive in character ($a = 0$). Switching multiplicative noise arrives at a -growth and non-contradicting representation of SOC demands increasing number of self-consistent equations: for example, within the field scheme [20] related to directed percolation ($a = 1/2$), mean-field approximation is applicable for dimensions more the critical magnitude $d_c = 4$; used here and in Refs. [17], [18] Lorenz scheme ($n = 3$) addresses to multiplicative noise characterized by the exponent $a = 1/3$ (see below).

Let us focus now on relation of above exponents to nonextensivity parameter q addressed to Tsallis definitions (57), (58) [24]. Relevant kinetic behavior could be described by non-linear Fokker-Planck equation

$$\mathcal{D}_t^\omega P(s, t) = \mathcal{D}_{-s}^2 P^q(s, t), \quad (79)$$

where measure units are chosen so that effective diffusion coefficient disappears, $\omega > 0$, $q > 0$ are relevant exponents [33], [34]. Supposing here normalized distribution function in self-similar form type of Eq. (2)

$$P(s, t) = s_c^{-1} \mathcal{P}(x); \quad s_c \equiv s_c(t), \quad x \equiv s/s_c, \quad (80)$$

we obtain

$$s_c^q \sim t^\omega, \quad \mathcal{P}^{q-1} \sim x. \quad (81)$$

On the other hand, we could use the fractional Fokker-Planck equation type of Eq. (71):

$$\mathcal{D}_t^\omega P(s, t) = \mathcal{D}_{-s}^{2\varpi} P(s, t). \quad (82)$$

Inserting here the solution (80), one finds dependencies

$$s_c^{2\varpi} \sim t^\omega, \quad \mathcal{P}^{2\varpi-1} \sim x, \quad (83)$$

whose comparison with Eqs. (81) yields

$$q = 2\varpi. \quad (84)$$

Because of the average $|s|$ in Eq. (72) is reduced to the scale s_c in the case of self-similar systems, relevant dependencies (73), (81) and (83) get

$$q = z\omega. \quad (85)$$

Combining this equality with Eqs. (75), (76) arrives at the resulting expression for nonextensivity parameter of the system under consideration:

$$q = \frac{2}{n(1-a)}. \quad (86)$$

Maximum magnitude $q = 2/n$ is related to systems with additive noise ($a = 0$), which is relevant to mean-field picture at number of governing equations $n < 2$ ($n = 1$, really). Switching multiplicative noise with increasing exponent $a > 0$ arrives at q -growth and self-organizing system becomes nonextensive in character ($q \geq 1$) at the boundary (78) of the mean-field applicability domain. In accordance with above estimation, fractional Lorenz system is nonextensive essentially if the exponent $a > 1/3$.

It is worthwhile to remember that we have addressed above the superdiffusion process only to be related to Lévy flights at discrete time instants with arbitrary displacements, including infinite ones [35]. Being related to the Fokker-Planck equation (71), such type processes are characterized by exponents $\omega = 1$ and $\varpi < 1$, the first of which is constant, whereas the second one characterizes fractal time-sequance of the Lévy flights to arrive at the dynamical exponent $z \equiv 2\varpi/\omega < 2$ (see the last of equations (73)). To be dependent on microscopic conditions, the probability distribution of displacements \mathbf{x} reads

$$p(\mathbf{x}) \sim x^{-(D+\gamma)} \quad (87)$$

that is characterized by the fractal dimension D and microscopic step exponent γ . It is appeared that in the case of rare events, when $\gamma < 2$, the dynamical exponent z is reduced to the microscopic step exponent ($z = \gamma < 2$), whereas at $\gamma \geq 2$ one has $z = 2$ [36].

In the opposite case of subdiffusion process, a microscopical ingredient is random Lévy walks instead of the discrete Lévy flights. This process is involved continuously in course of the time over discrete placed traps, so that the exponents $\omega < 1$ addresses fractal properties of this space to be dependent on microscopic conditions. This properties produce transformation of the usual Boltzmann-Gibbs statistics in nonextensive manner [24]. Along this line, the subdiffusion process is presented by the Tsallis-type distribution [37]

$$p(\mathbf{x}) \propto [1 + \beta(q-1)x^2]^{-\frac{1}{q-1}}, \quad \beta = \text{const} > 0, \quad (88)$$

where deviation $q-1$ of the nonextensive parameter is caused by fractal nature of the system phase space to be connected with the step exponent γ as follows:

$$q = 1 + \frac{2}{D + \gamma}. \quad (89)$$

Formal advantage of the distribution (88) is that corresponding q -weighted average

$$\langle \mathbf{x}^2 \rangle_q \equiv \int \mathbf{x}^2 p^q(\mathbf{x}) d^D x, \quad (90)$$

where the integrand varies as $x^{-(1+\gamma)}$, is converges for arbitrary step exponents $\gamma > 0$. As a result, the law of motion of the random Lévy walker is given by

$$\langle \mathbf{x}^2 \rangle_q \sim t^\omega, \quad \omega = \begin{cases} q-1 & \text{at } \gamma, q < 2, \\ 1 - (q-1)\frac{D}{2} & \text{at } \gamma \geq 2, q > 1. \end{cases} \quad (91)$$

In contrast to Eq. (83), where the exponents $\varpi < 1$, $\omega = 1$ are relevant to the superdiffusion, here one has inverted relations $\varpi = 1$, $\omega < 1$. Thus, in accordance with subdiffusion nature, the last equality (73) yields the dynamical exponent $z > 2$.

In general case $\varpi, \omega \neq 1$, inserting Eqs. (91) into the relation (85) arrives at the result

$$z = \begin{cases} \frac{q}{1 - \frac{D}{2}(q-1)} & \text{at } 1 < q \leq q_D, \\ \frac{q}{q-1} & \text{at } q_D \leq q \leq 2, \end{cases} \quad (92)$$

where boundary value of the nonextensivity parameter is introduced:

$$q_D \equiv \frac{4 + D}{2 + D}. \quad (93)$$

To avoid a mistake, let us focus that in contrast to equalities (1), (74), (75), which could be addressed to both the real phase space and the configurational one (the latter is spanned by variables of governing equations), above obtained relations (91) – (93) are relevant to the real phase space only. This is reflected by addressing the fractal dimension D to the only real coordinate space in the former case, whereas in the latter it is reduced to the effective

value (76). Along the principle line of our treatment, central role is played by the relation (76) since, by analogy with studying renormalization group, we have considered mainly the properties of the configurational space but not real diffusion process.

Finally, let us address the question: Why the Lorenz system is used but not Rössler one or another? The reason can be recognized within supersymmetry field approach, whose using shows that the Lorenz system could be generated by the Langevin equation for order parameter to be relevant to standard stochastic system [38]. On the other hand, one can see within microscopic consideration that Lorenz system addresses to the simplest Hamiltonian of a bozon-fermion system [39]. To convince in this statement, let us consider such system with interaction w . Bozons are described by creation and annihilation operators b_l^+ , b_l , satisfying the usual commutation relation: $[b_l, b_m^+] = \delta_{lm}$, where l, m are the site numbers. The two-level Fermion subsystem is represented by operators $a_{l\alpha}^+$, $a_{l\alpha}$, $\alpha = 1, 2$, for which the anti-commutation relation $\{a_{l\alpha}, a_{m\beta}^+\} = \delta_{lm}\delta_{\alpha\beta}$ is fulfilled. The occupation numbers $b_{\mathbf{k}}^+ b_{\mathbf{k}}$ determine the Bozon distribution within \mathbf{k} -representation that corresponds to the Fourier transform over lattice sites l . To represent the Fermi subsystem we should introduce the operator $d_l \equiv a_{l1}^+ a_{l2}$ determining the polarization with respect to the saturation over levels $\alpha = 1, 2$, as well as the occupation numbers $n_{l\alpha} \equiv a_{l\alpha}^+ a_{l\alpha}$. As a result, behavior of the system is defined by Dicke Hamiltonian

$$H = \sum_{\mathbf{k}} \left\{ (E_1 n_{\mathbf{k}1} + E_2 n_{\mathbf{k}2}) + \omega_{\mathbf{k}} b_{\mathbf{k}}^+ b_{\mathbf{k}} + \frac{i}{2} w (b_{\mathbf{k}}^+ d_{\mathbf{k}} - d_{\mathbf{k}}^+ b_{\mathbf{k}}) \right\}, \quad (94)$$

where $E_{1,2}$ are energies of the Fermi levels, $\omega_{\mathbf{k}}$ is the Bozon dispersion law, the imaginary unit before the interaction w reflects the Hermitian property and the Planck constant is $\hbar = 1$.

The Heisenberg equations of motion corresponding to Hamiltonian (94) have the form

$$\dot{b}_{\mathbf{k}} = -i\omega_{\mathbf{k}} b_{\mathbf{k}} + \frac{w}{2} d_{\mathbf{k}}; \quad (95)$$

$$\dot{d}_{\mathbf{k}} = -i\Delta d_{\mathbf{k}} + \frac{w}{2} b_{\mathbf{k}} (n_{\mathbf{k}2} - n_{\mathbf{k}1}), \quad \Delta \equiv E_2 - E_1; \quad (96)$$

$$\dot{n}_{\mathbf{k}1} = \frac{w}{2} (b_{\mathbf{k}}^+ d_{\mathbf{k}} + d_{\mathbf{k}}^+ b_{\mathbf{k}}), \quad \dot{n}_{\mathbf{k}2} = -\frac{w}{2} (b_{\mathbf{k}}^+ d_{\mathbf{k}} + d_{\mathbf{k}}^+ b_{\mathbf{k}}). \quad (97)$$

At condition of resonance, the first terms in the right hand sides of equations (96), (97) containing frequencies $\omega_{\mathbf{k}}$ and Δ may be suppressed by introducing the multipliers $\exp(-i\omega_{\mathbf{k}}t)$ and $\exp(-i\Delta t)$ for the time dependencies $b_{\mathbf{k}}(t)$, $d_{\mathbf{k}}(t)$, respectively. On the other hand, to take into account the dissipation, these frequencies acquire imaginary additions $-i/\tau_x$, $-i/\tau_y$ characterized by relaxation times τ_x , τ_y (here the conditions $\text{Im } \omega_{\mathbf{k}} < 0$, $\text{Im } \Delta < 0$ reflect the causality principle). As a result, equations (96), (97) get the dissipative terms $-b_{\mathbf{k}}/\tau_x$, $-d_{\mathbf{k}}/\tau_y$, where τ_x is the relaxation time of Bozon distribution and τ_y is the Fermion polarization time. Obviously, one can suppose that the dissipation influences onto the Fermi levels occupancies $n_{\mathbf{k}\alpha}(t)$ also. However, since the stationary values $n_{\mathbf{k}\alpha}^0 \neq 0$ (in case of external drive $n_{\mathbf{k}2}^0 > n_{\mathbf{k}1}^0$) the dissipative terms in Eqs. (97) take much complicated form: $-(n_{\mathbf{k}\alpha} - n_{\mathbf{k}\alpha}^0)/\tau_S$, where τ_S is the relaxation time of the Fermion distribution over levels $\alpha = 1, 2$.

Now, let us introduce the macroscopic quantities

$$\begin{aligned}
u_{\mathbf{k}} &\equiv \langle b_{\mathbf{k}}^+ \rangle = \langle b_{\mathbf{k}} \rangle, & v_{\mathbf{k}} &\equiv \langle d_{\mathbf{k}} \rangle = \langle d_{\mathbf{k}}^+ \rangle, \\
S_{\mathbf{k}} &\equiv \langle n_{\mathbf{k}2} - n_{\mathbf{k}1} \rangle, & S_{\mathbf{k}}^0 &\equiv \langle n_{\mathbf{k}2}^0 - n_{\mathbf{k}1}^0 \rangle,
\end{aligned}
\tag{98}$$

where the angular brackets mean thermodynamical averaging. Then, neglecting the correlation in distribution of particles over quantum states and omitting dependence on the wave vector \mathbf{k} , the Heisenberg equations (96) – (97), being complemented by dissipative terms, result in the initial Lorenz system (6), (8), (9), whose parameters take magnitudes $a = 1$, $\tau_x = 2/w$, $D = (2w)^{-1}$. Respectively, the dimensionless variables in the system (10) – (12) are as follows: $u = w(\tau_y\tau_S)^{1/2}\dot{x}$, $v = w(\tau_y\tau_S)^{1/2}\dot{y}$ and $S = (w\tau_y/2)y'$.

As a result, we arrive at the conclusion that Lorenz system is relevant microscopically to the simplest bozon-fermion system defined by Dicke Hamiltonian (94). At first glance, it could have been shown that one can write corresponding expression for macroscopic (effective) Hamiltonian being a synergetic potential, whose dependence on the freedom degrees u , v , S could have generated the Lorenz system. But such dependence is appeared to be absent because of the effective Hamiltonian has to take into account quite different commutation rules related to different freedom degrees. Obvious advantage of above mentioned supersymmetry theory [38] and stated microscopic approach is that we have explicit possibility to account such difference. Generally, this situation is relevant to known problem of description of systems with intermediate statistics (see Ref. [40]).

VII. ACKNOWLEDGMENTS

We would like to dedicate this paper to the memory of our friend and colleague Dr. Evgeny Toropov, whose activity had prompted this work.

VIII. APPENDIX

Here the basic properties of fractional integral and derivative, as well as Jackson derivative are quoted for convenience. The integral of fractional order ϖ is defined by equality [30], [31]

$$\mathcal{I}_x^\varpi f(x) \equiv \frac{1}{\Gamma(\varpi)} \int_0^x \frac{f(x')}{(x-x')^{1-\varpi}} dx', \quad \varpi > 0,
\tag{A.1}$$

where $f(x)$ is arbitrary function, $\Gamma(x)$ is standard Gamma-function. To be inverted to the fractional integral, relevant derivative $\mathcal{D}_x^\varpi \equiv \mathcal{I}_x^{-\varpi}$ of order $\varpi > 0$ is determined as follows:

$$\mathcal{D}_x^\varpi f(x) \equiv \frac{1}{\Gamma(-\varpi)} \int_0^x \frac{f(x')}{(x-x')^{1+\varpi}} dx'.
\tag{A.2}$$

At $0 < \varpi < 1$ it is convenient to use equation

$$\mathcal{D}_x^\varpi f(x) \equiv \frac{\varpi}{\Gamma(1-\varpi)} \int_0^x \frac{f(x) - f(x')}{(x-x')^{1+\varpi}} dx',
\tag{A.3}$$

where we take into account known equality $x\Gamma(x) = \Gamma(x+1)$ for $x \equiv -\varpi$.

Let us introduce now Jackson q -derivative, whose advantage for analyzing self-similar system is that this derivative determines the rate of a function $f(x)$ variation with respect to dilatation $q \neq 1$, but not to the shift $dx \rightarrow 0$, as in usual case $q = 1$. According to such definition, Jackson q -derivative reads:

$$\mathcal{D}_q f(x) \equiv \frac{f(qx) - f(x)}{q - 1}, \quad q > 0. \quad (\text{A.4})$$

For important case of homogeneous function, being subjected to condition

$$f(qx) \equiv q^\alpha f(x), \quad (\text{A.5})$$

where $q > 0$ is a dilatation parameter and $\alpha > 0$ is an exponent, the Jackson q -derivative is reduced to Jackson q -number:

$$\mathcal{D}_q f(x) = [\alpha]_q f(x), \quad [\alpha]_q \equiv \frac{\alpha^q - 1}{q - 1}. \quad (\text{A.6})$$

It is easily to see that the value $[\alpha]_q \rightarrow \alpha$ in the limit $q \rightarrow 1$ and varies as $q^{\alpha-1}$ at $q \rightarrow \infty$. On the other hand, the Tsallis q -logarithmic function

$$\ln_q x \equiv \frac{x^{q-1} - 1}{q - 1} \quad (\text{A.7})$$

can be represented in the form of the Jackson q -number (A.6) with the index $\alpha = (q - 1)(\ln x / \ln q)$. Accompanied by Eqs. (A.6) this relation and obvious equality

$$\ln_q(xy) = \ln_q x + \ln_q y + (q - 1)(\ln_q x)(\ln_q y) \quad (\text{A.8})$$

lead to important rule for the Jackson derivative:

$$\mathcal{D}_q [f(x)g(x)] = [\mathcal{D}_q f(x)] g(x) + f(x) [\mathcal{D}_q g(x)] + (q - 1) [\mathcal{D}_q f(x)] [\mathcal{D}_q g(x)]. \quad (\text{A.9})$$

Generalizing Eqs. (A.3), (A.4), let us introduce finally a fractional ϖ -derivative:

$$\mathcal{D}^\varpi f(x) \equiv \frac{\varpi x^{-\varpi}}{\Gamma(1 - \varpi)} \int_0^1 \frac{f(x) - f(qx)}{(1 - q)^{1+\varpi}} dq, \quad 0 < \varpi < 1. \quad (\text{A.10})$$

In the case of self-similar system, the function $f(x)$ is homogeneous to be subjected to condition (A.5). Then, the definition (A.10) is simplified:

$$\mathcal{D}^\varpi f(x) \equiv \{\alpha\}_\varpi x^{-\varpi} f(x), \quad 0 < \varpi < 1 \quad (\text{A.11})$$

to be reduced to fractional ϖ -number

$$\{\alpha\}_\varpi \equiv \frac{\varpi}{\Gamma(1 - \varpi)} \int_0^1 \frac{1 - q^\alpha}{(1 - q)^{1+\varpi}} dq, \quad 0 < \alpha, \quad 0 < \varpi < 1. \quad (\text{A.12})$$

Being the combination of Γ -functions:

$$\{\alpha\}_{\varpi} = \frac{\Gamma(\alpha + 1)}{\Gamma(\alpha + 1 - \varpi)} - \frac{1}{\Gamma(1 - \varpi)}, \quad (\text{A.13})$$

this number increases monotonically with growth of both exponents α and ϖ taking zeroth magnitude on the axes $\varpi = 0$, $\alpha = 0$ and characteristic values $\left\{\frac{1}{2}\right\}_{\frac{1}{2}} = \frac{\sqrt{\pi}}{2} - \frac{1}{\sqrt{\pi}} \simeq 0.322$, $\{1\}_1 = 1$. Such behavior is characterized by the particular dependencies

$$\{\alpha\}_{\varpi} = \begin{cases} \alpha & \text{at } \varpi = 1, \\ \Gamma(1 + \alpha) - \frac{1}{\Gamma(1-\alpha)} & \text{at } \varpi = \alpha, \\ \frac{\varpi}{\Gamma(2-\varpi)} & \text{at } \alpha = 1. \end{cases} \quad (\text{A.14})$$

Thus, if q -number (A.6) related to Jackson derivative (A.4) tends to exponent α in the limit $q \rightarrow 1$, ϖ -number (A.12) corresponding to fractional integral (A.10) is reduced to factor α at $\varpi = 1$.

- [1] P. Bak, *How Nature Works: the Science of Self-Organized Criticality* (Oxford University Press, Oxford, 1997).
- [2] H. J. Jensen, *Self-Organized Criticality. Emergent Complex Behavior in Physical and Biological Systems*, in: *Cambridge Lecture Notes in Physics* (Cambridge University Press, Cambridge, 1998).
- [3] M. Parzuski, S. Maslov, P. Bak, *Phys. Rev.* **E53** (1996) 414.
- [4] S. F. Edwards, D. R. Wilkinson, *Proc. Roy. Soc.* **A381** (1982) 17.
- [5] A. Mehta, G. C. Barker, *Rep. Prog. Phys.* (1994) 383.
- [6] J.-P. Bouchaud, M. E. Cates, J. R. Prakash, S. F. Edwards *J. Phys. I (France)* **4** (1994) 1383.
- [7] K. P. Haderler, C. Kuttler, *Granular Matter* **2** (1999) 9.
- [8] P. Bak, K. Sneppen, *Phys. Rev. Lett.* **71** (1993) 4083.
- [9] T. Halpin-Healy, Y.-C. Zhang, *Phys. Rep.* **254** (1995) 215.
- [10] D. Dhar, R. Ramaswamy, *Phys. Rev. Lett.* **63** (1989) 1659; D. Dhar, *ibid.* **64** (1991) 1613.
- [11] L. Pietronero, A. Vespignani, S. Zapperi, *Phys. Rev. Lett.* **72** (1994) 1690; *Phys. Rev.* **E51** (1995) 1711.
- [12] P. Bak, C. Tang, K. Wiesenfeld, *Phys. Rev. Lett.* **59** (1987) 381.
- [13] L. P. Kadanoff, S. R. Nagel, L. Wu, S. Zhu, *Phys. Rev.* **A39** (1989) 6524.
- [14] P. Grassberger, S. S. Manna, *J. Phys. (France)* **51** (1990) 1077.
- [15] T. Hwa, M. Kadar, *Phys. Rev.* **A45** (1992) 7002.
- [16] L. Gil, D. Sornette, *Phys. Rev. Lett.* **76** (1996) 3991.
- [17] A.I. Olemskoi, A.V. Khomenko, *JETP* **83** (1996) 1180.
- [18] A. I. Olemskoi, A. V. Khomenko, *Phys. Rev.* **E63** (2001) 036116.
- [19] A. Vespignani, S. Zapperi, *Phys. Rev. Lett.* **78** (1997) 4793; *Phys. Rev.* **E57** (1998) 6345.
- [20] A. Vespignani, R. Dickman, M. A. Muñoz, S. Zapperi, *Phys. Rev. Lett.* **81** (1998) 5676; *Phys. Rev.* **E62** (2000) 4564.

- [21] J. Zinn-Justin, *Quantum Field Theory and Critical Phenomena* (Clarendon Press, Oxford, 1993).
- [22] S. F. Edwards, R. B. S. Oakeshott, *Physica* **A157** (1989) 1080.
- [23] S. F. Edwards, in: *Granular Matter: An Interdisciplinary Approach*, A. Metha, Ed. (Springer-Verlag, New-York, 1994).
- [24] C. Tsallis, in: *Lecture Notes in Physics*, S. Abe, Y. Okamoto, Eds. (Springer-Verlag, Heidelberg, 2001).
- [25] G. M. Zaslavsky, *Chaos* **4** (1994) 25; *Physica* **D76** (1994) 110; A. I. Saichev, G. M. Zaslavsky, *Chaos* **7** (1997) 753.
- [26] H. Risken, *The Fokker-Planck equation* (Springer, Berlin, 1989).
- [27] G. Haken, *Synergetics, an Introduction* (Springer, Berlin, 1983).
- [28] A.I. Olemskoi, *Physics-Uspekhi*, **41**, 269 (1998).
- [29] M. Cencini, M. Falcioni, E. Olbrich, H. Kantz, A. Vulpiani, *Phys. Rev.* **E62** (2000) 427.
- [30] S.G. Samko, A.A. Kilbas, O.I. Marichev, *Fractional integrals and derivatives – theory and applications* (Gordon and Breach, New-York, 1993).
- [31] *Applications of Fractional Calculus in Physics*, R. Hilfer, Ed. (World Scientific, Singapore, 2000).
- [32] A. Chessa, E. Marinari, A. Vespignani, S. Zapperi, *Phys. Rev.* **E57** (1998) R6241.
- [33] A. I. Olemskoi, *JETP Let.* **71** (2000) 285.
- [34] A. I. Olemskoi, D. O. Kharchenko, *Physica* **A293** (2001) 178.
- [35] J.-P. Bouchaud, A. Georges, *Phys. Rep.* **195** (1991) 127.
- [36] H. C. Fogedby, *Phys. Rev.* **E58** (1998) 1690.
- [37] D. H. Zanette, P. A. Alemany, *Phys. Rev. Lett.* **75** (1995) 366.
- [38] A.I. Olemskoi, A.V. Khomenko, cond-mat/0008121.
- [39] A. I. Olemskoi, *Theory of Structure Transformations in Non-Equilibrium Condensed Matter* (NOVA Science, New-York, 1999).
- [40] G. Kaniadakis, cond-mat/0103467.

FIGURE CAPTIONS

Fig. 1. The S_0 -dependencies of (a) the velocities u_e , u^m , and (b) the equilibrium slope S_e . The arrows indicate the hysteresis loop.

Fig. 2. Phase portraits in the $v - u$ plane at $m = 1$, $u_0 = 0.1$, $S_0 = 1.25S_c$: (a) $\epsilon = 10^{-2}$; (b) $\epsilon = 1$; (c) $\epsilon = 10^2$.

Fig. 3. Phase diagrams at fixed values I_v : (a) $I_v = 0$; (b) $I_v = 1$; (c) $I_v = 2$. Curves 1 and 2 define the boundary of stability of avalanche (A) and non-avalanche (N) phases.

Fig. 4. Phase diagram for system with $S_0 = 0$ and I_s , $I_v \neq 0$ (D – disordering point; T – tricritical point; C – critical point).

Fig. 5. The S_0 -dependence of the steady-state velocity u at $a = 0, 0.5, 0.7, 0.9, 1.0$ from top to bottom.

Fig. 6. The S_0 -dependence of the steady-state velocity u : (a) at $a = 0.75$, $I_v = 1$ (curves 1 – 4 address to $I_S = 1, 2, 3, 5$); (b) at $I_v = 1$, $I_S = 5$ (curves 1 – 4 address to $a = 0.25, 0.5, 0.75, 1.0$).

Fig. 7. Three-dimensional phase diagram (the non-avalanche domain is located under surface).

Fig. 8. Phase diagram for system with $S_0 = 0$ and I_s , $I_v \neq 0$ at $a = 0.5, 0.75, 1.0$ (dotted, solid and dashed curves, respectively). Diamonds address to curves 1 – 4 in Fig. 11.

Fig. 9. Phase diagram in the $I_S - a$ plane at $I_v = 2, 3, 4, 5, 6$ from bottom to top (the non-avalanche domain is located inside the curves).

Fig. 10. The energy dependences of the avalanche ensemble temperatures: (a) nonstationary magnitude T versus ratio $\bar{\zeta}_q/\zeta^0$; (b) stationary temperature T_0 versus ζ^0 .

Fig. 11. Distribution function (68) at $\tau = 1.5$ and regimes pointed out by diamonds in Fig. 8: 1) $I_v = 0$, $I_S = 50$ (SOC); 2) $I_v = 0.5$, $I_S = 30$ (A+N); 3) $I_v = 1$, $I_S = 5$ (N); 4) $I_v = 2$, $I_S = 0.5$ (A).

Fig. 12. Deviation $\delta\tau$ of the linear slope of curve 1 depicted in Fig. 11 from parameter τ versus the exponent τ itself ($I_S = 10, 50, 10^3$ from bottom to top).

Fig. 13. Dependences of exponent τ : (a) on equations number n ($a = 0, \frac{1}{3}, \frac{1}{2}, \frac{2}{3}$ from top to bottom); (b) on exponent a ($n = 2, 3, 4, 6, 8, 10$ from bottom to top); (c) phase diagram for mean-field and nonextensivity domains.

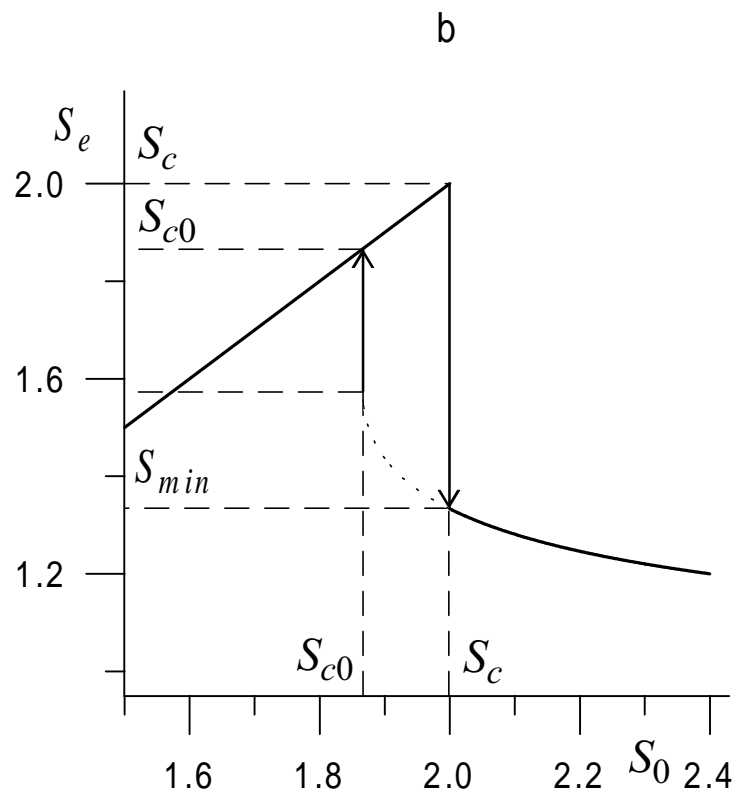
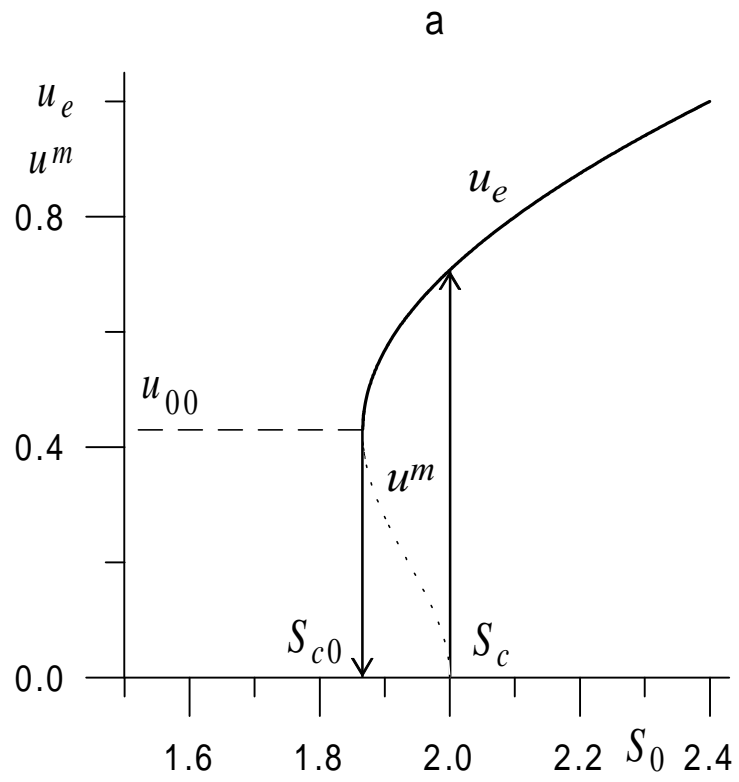


Fig. 1

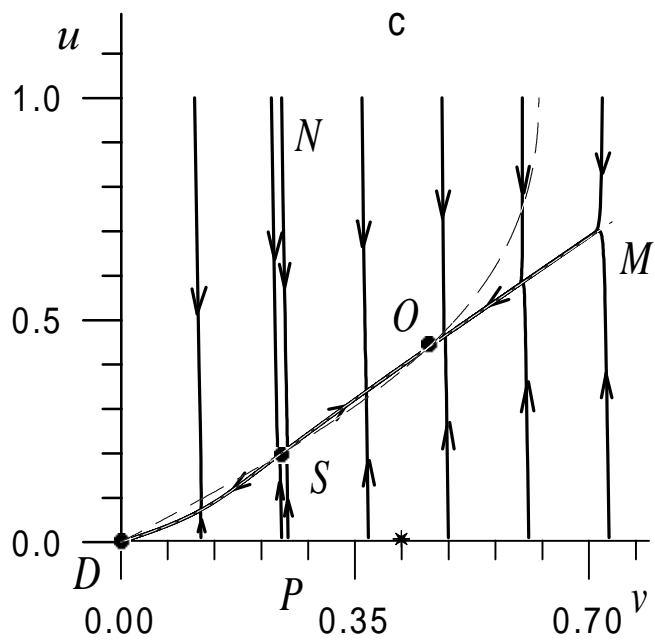
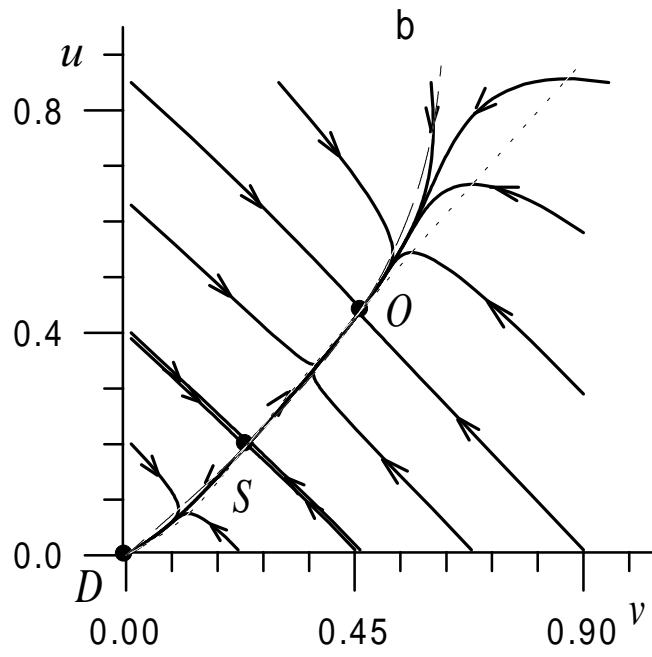
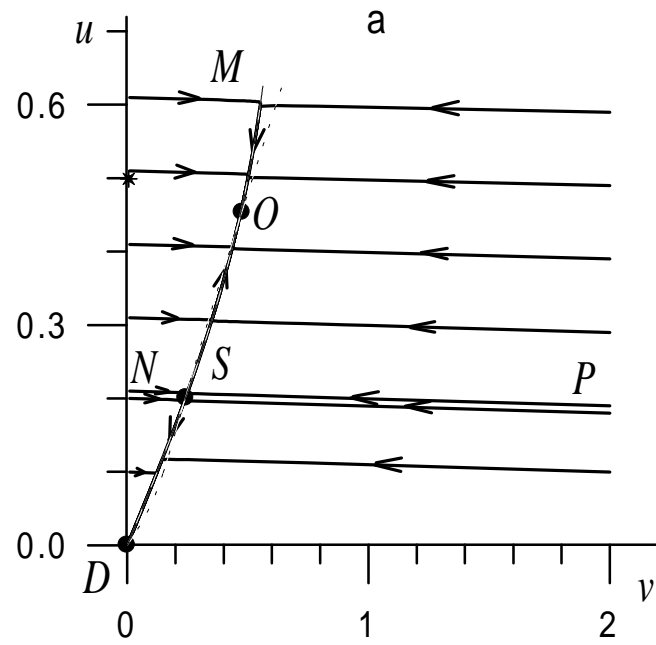


Fig. 2

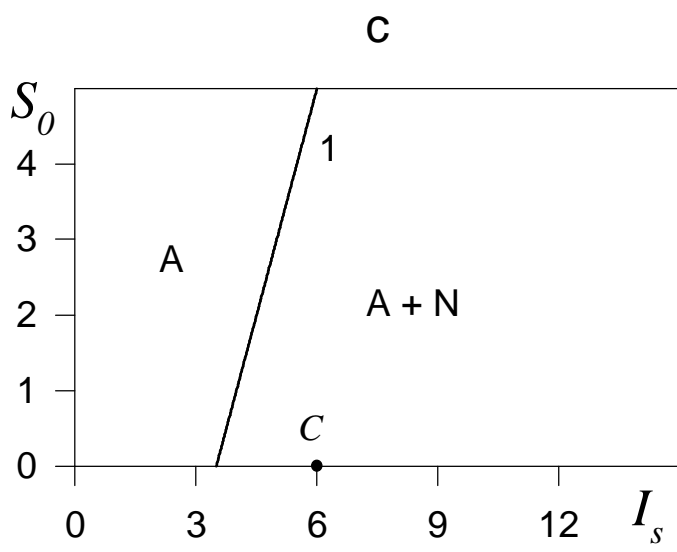
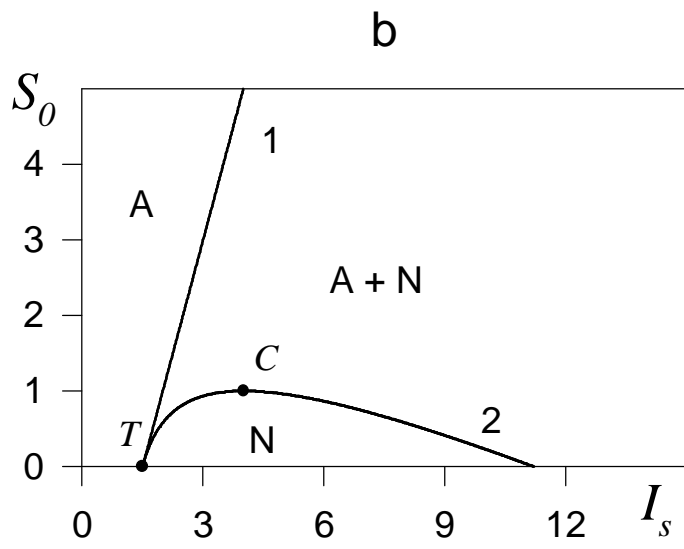
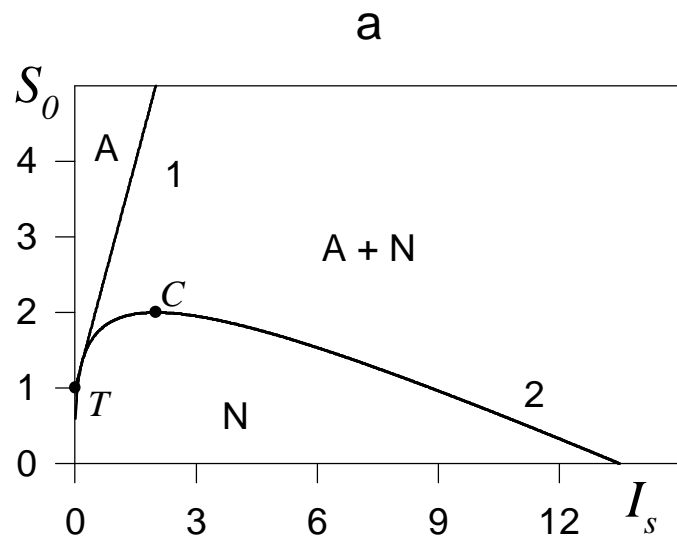


Fig.3

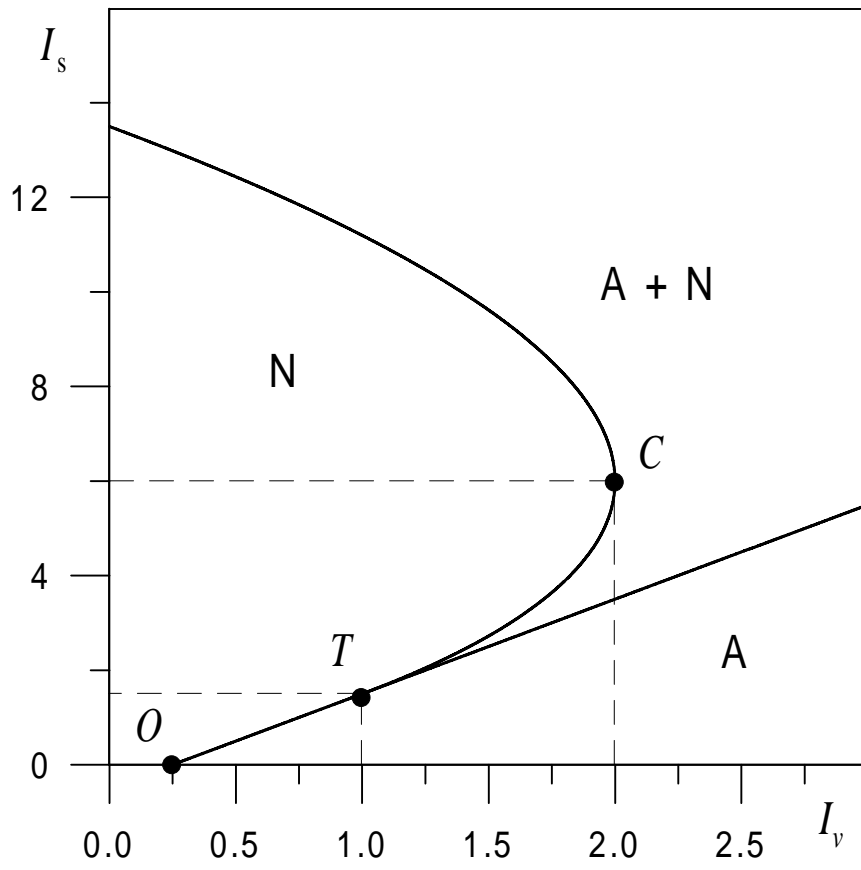


Fig. 4

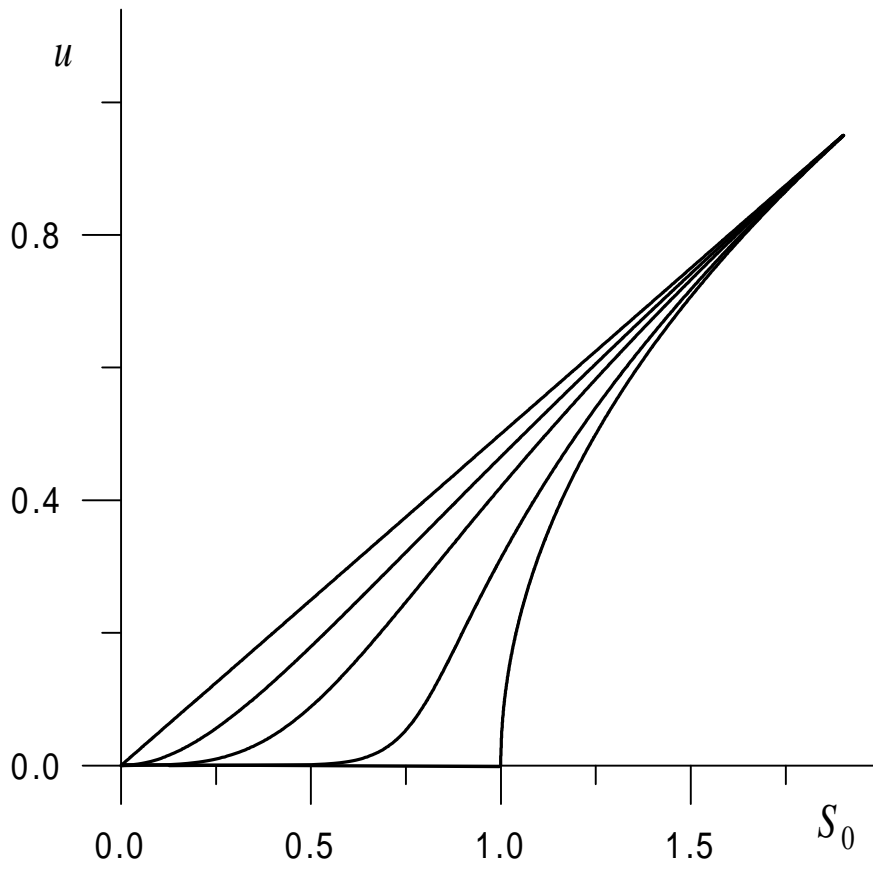
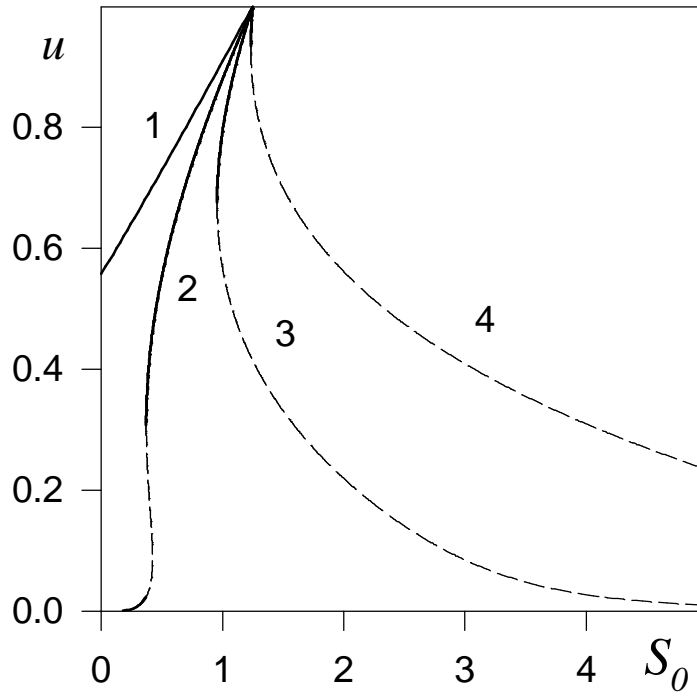


Fig. 5

a



b

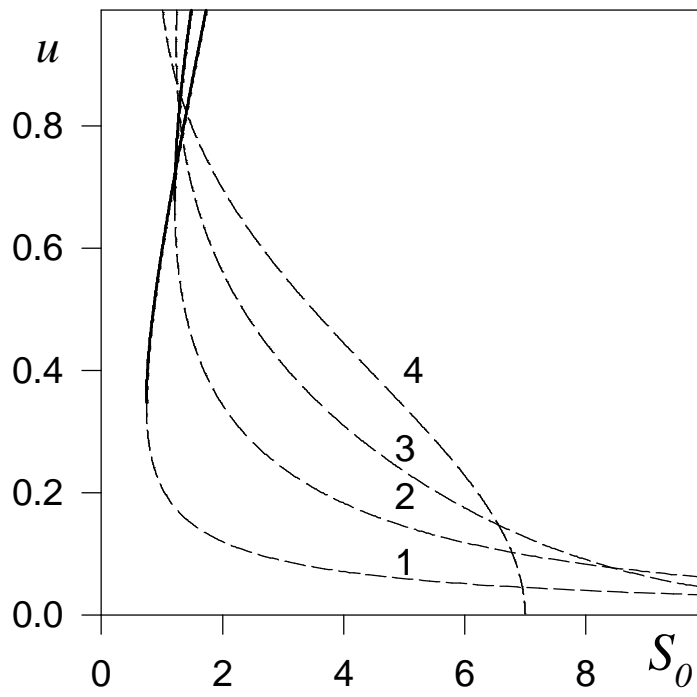


Fig. 6

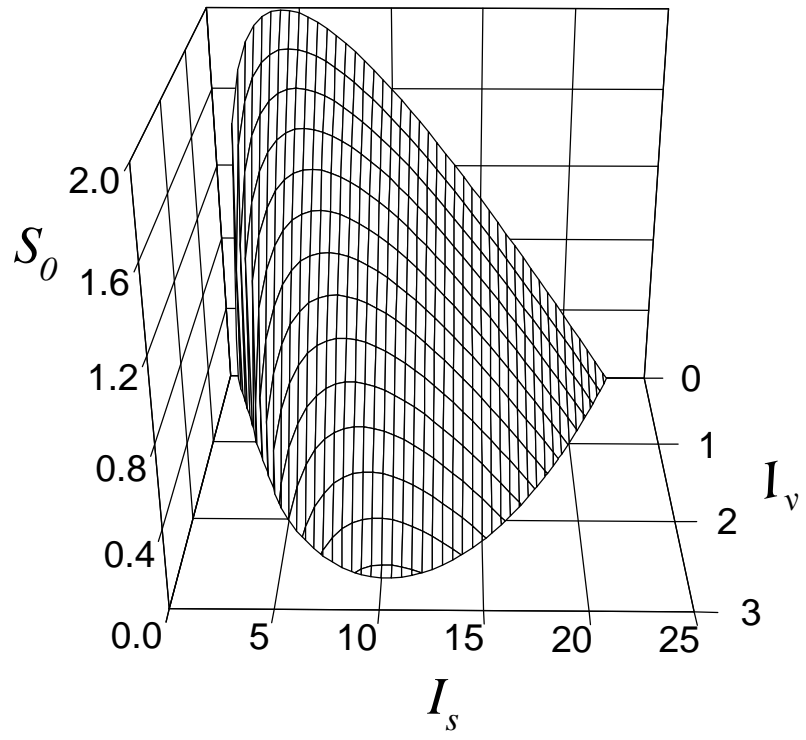


Fig. 7

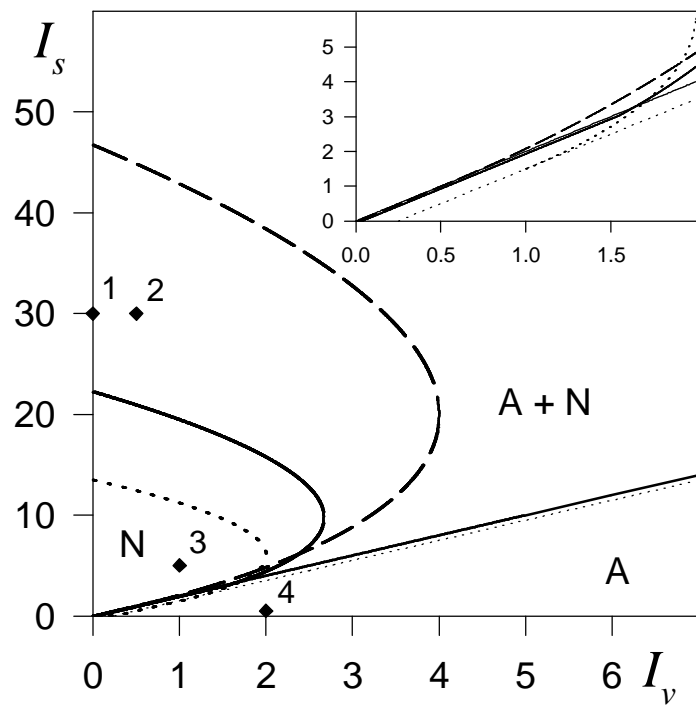


Fig. 8

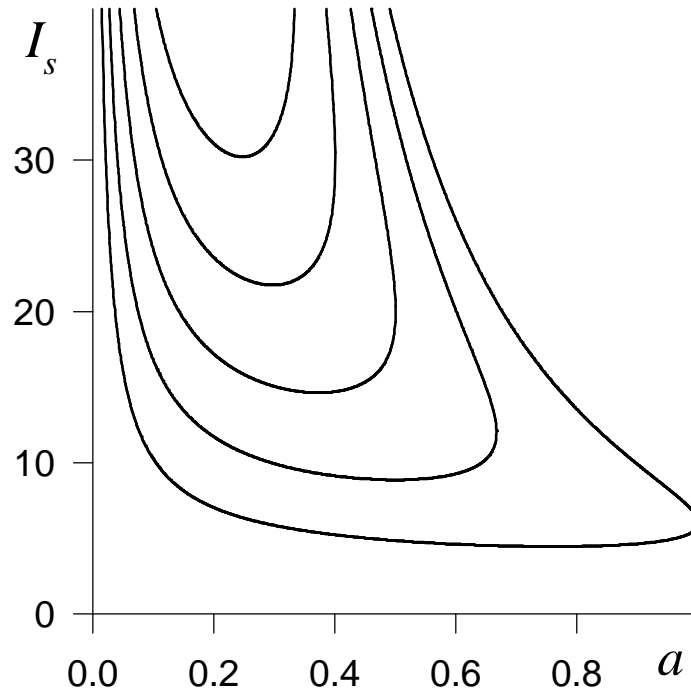
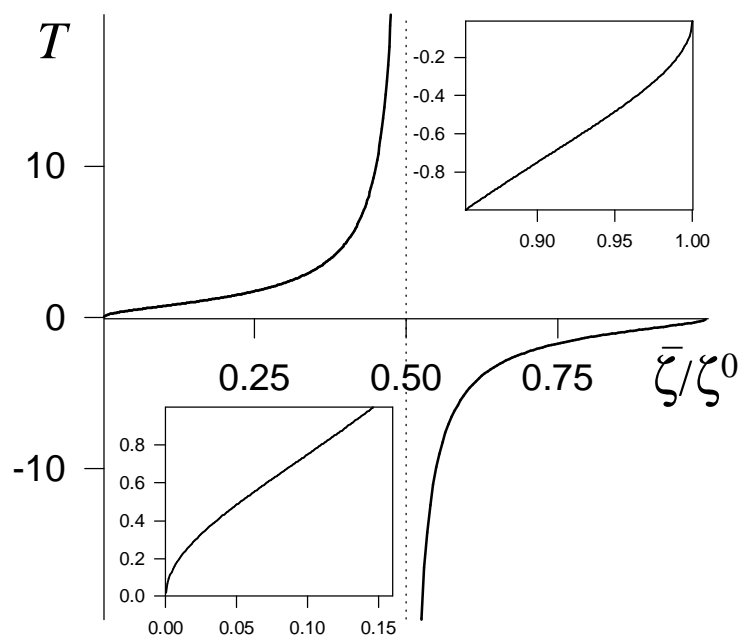


Fig. 9

a



b

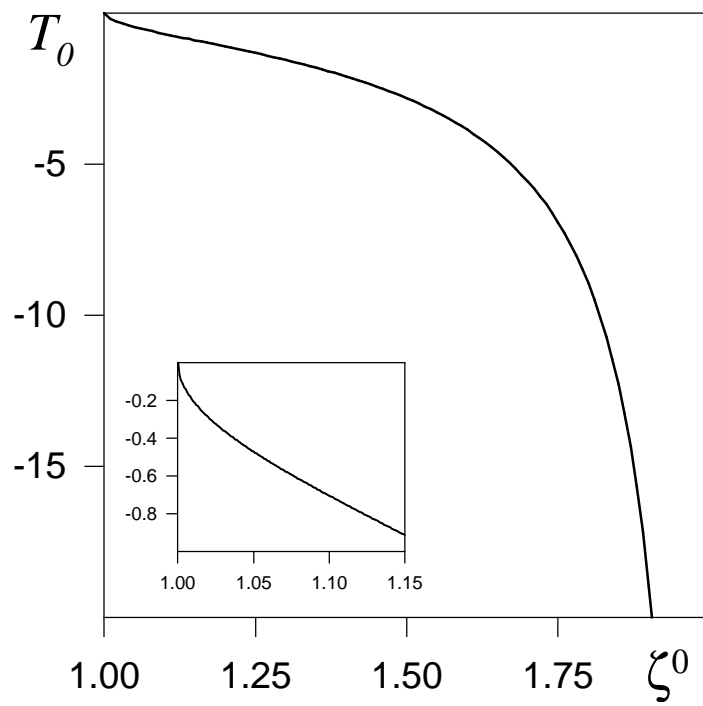


Fig.10

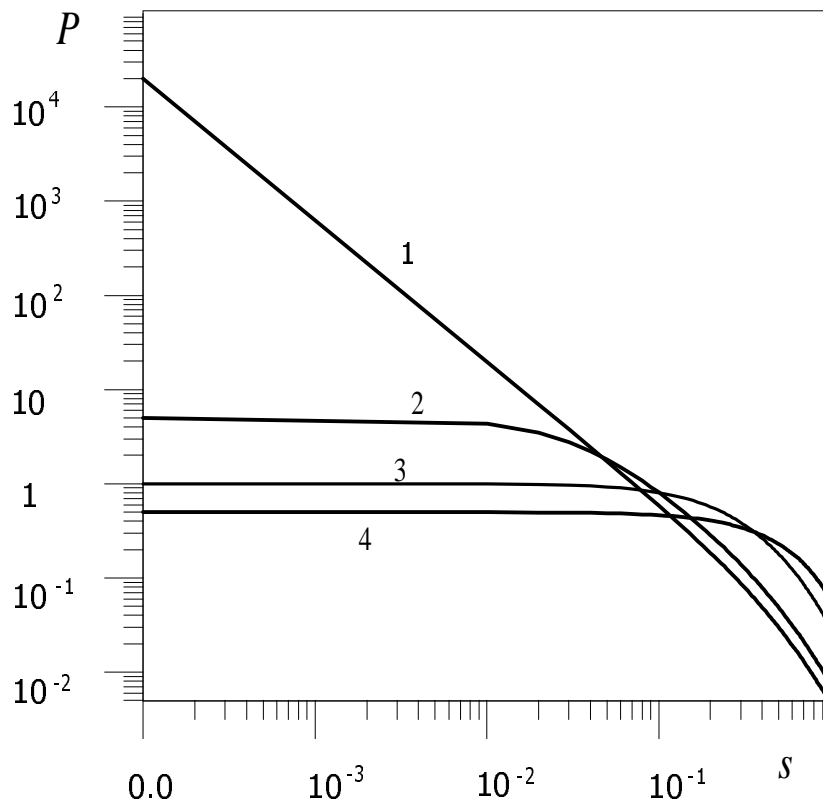


Fig. 11

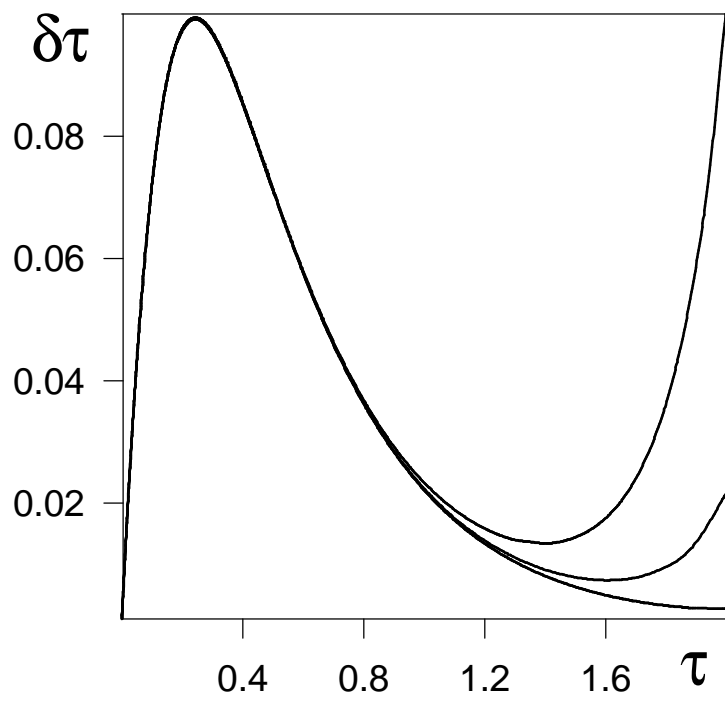


Fig.12

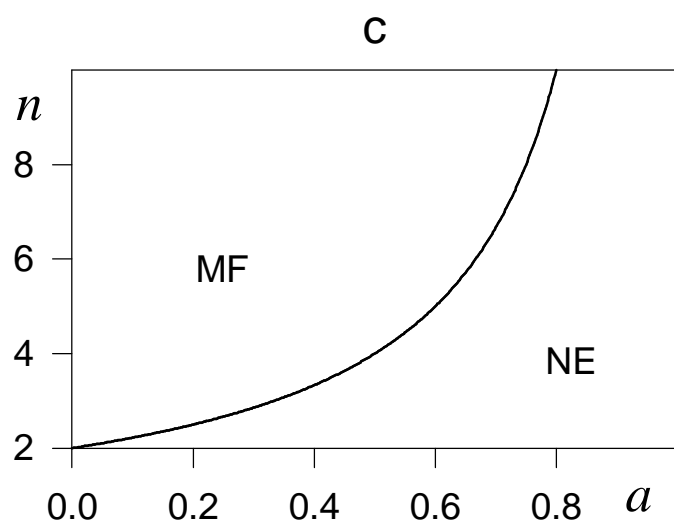
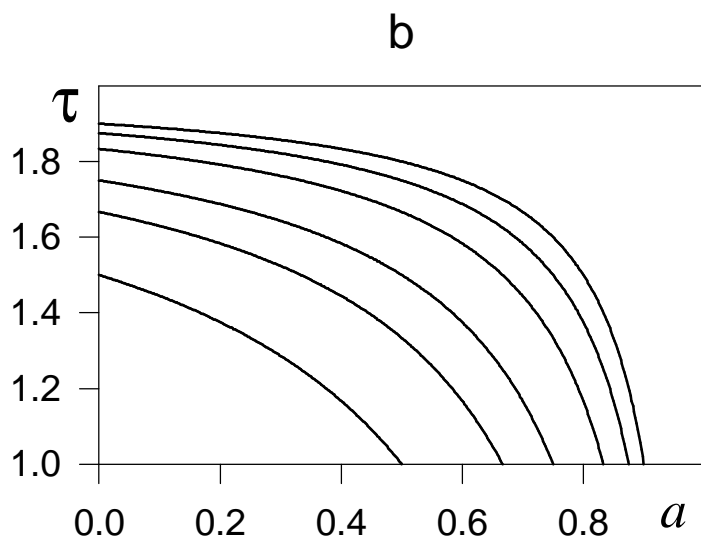
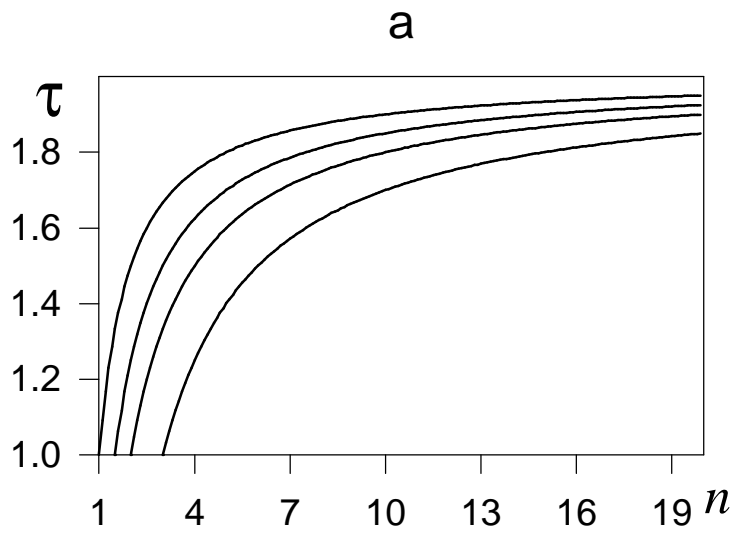


Fig.13